THE JOURNAL OF COMPARATIVE NEUROLOGY 411:97–118 (1999)

Projection Patterns of Single Mossy Fibers Originating From the Lateral Reticular Nucleus in the Rat Cerebellar Cortex and Nuclei

H.-S. WU, I. SUGIHARA, AND Y. SHINODA*
Department of Physiology, School of Medicine, Tokyo Medical and Dental University, Bunkyo-ku, Tokyo, 113–8519, Japan

ABSTRACT

Projection of neurons in the lateral reticular nucleus (LRN) to the cerebellar cortex (Cx) and the deep cerebellar nuclei (DCN) was studied in the rat by using the anterograde tracer biotinylated dextran amine (BDA). After injection of BDA into the LRN, labeled terminals were seen bilaterally in most cases in the vermis, intermediate zone, and hemisphere of the anterior lobe, and in various areas in the posterior lobe, except the flocculus, paraflocculus, and nodulus. Areas of dense terminal projection were often organized in multiple longitudinal zones. The entire axonal trajectory of single axons of labeled LRN neurons was reconstructed from serial sections. Stem axons entered the cerebellum through the inferior cerebellar peduncle (mostly ipsilateral), and ran transversely in the deep cerebellar white matter. They often entered the contralateral side across the midline. Along the way, primary collaterals were successively given off from the transversely running stem axons at almost right angles to the Cx and DCN, and individual primary collaterals had longitudinal arborizations that terminated as mossy fibers in multiple lobules of the Cx. These collaterals arising from single LRN axons terminated bilaterally or unilaterally in the vermis, intermediate area, and sometimes hemisphere, and in different cerebellar and vestibular nuclei simultaneously. The cortical terminals of single axons appeared to be distributed in multiple longitudinal zones that were arranged in a mediolateral direction. All of the LRN axons examined (n = 29) had axon collaterals to the DCN. All of the terminals observed in the DCN and vestibular nuclei belonged to axon collaterals of mossy fibers terminating in the Cx. J. Comp. Neurol. 411:97–118, 1999.

Indexing terms: afferent pathways; cerebellar cortex; deep cerebellar nuclei; nerve endings; medulla oblongata

Mossy fibers in the cerebellar cortex (Cx) are characterized by their thickened ends, which resemble a piece of moss in the granular layer of the Cx (Ramón y Cajal, 1911). Afferents of the cerebellum from many different origins, including brainstem precerebellar nuclei but excluding the inferior olive (IO), take the form of mossy fibers in the Cx. Due to the uniformity of the local circuit of the Cx, the projection pattern of afferents to the Cx, including the mossy fiber system, plays a significant role in determining the functional compartmentation and organized action of the cerebellum (Eccles et al., 1967; Palay and Chan-Palay, 1974; Ito, 1984).

Classic studies on receptive field organization in the Cx have shown the existence of transversely organized divisions (Snider, 1950; Grant, 1962; Brodal, 1981). On the other hand, more recent studies on mapping receptive fields through olivocerebellar climbing fiber projection have suggested that the Cx is composed of many longitudinal functional compartments (Andersson and Oscarsson, 1978; Ito et al., 1982; Ito, 1984). This electrophysiologically defined organization is consistent with the anatomically defined longitudinal compartments in the Cx (Groenewe-

Grant sponsor: CREST (Core Research for Evolutional Science and Technology) of the Japan Science and Technology Corporation; Grant sponsor: Ministry of Education, Science, and Culture of Japan; Grant sponsor: Sasakawa Health Science Foundation; Grant sponsor: Iwaki Scholarship Foundation.

*Correspondence to: Dr. Yoshikazu Shinoda, Department of Physiology, School of Medicine, Tokyo Medical and Dental University, 1–5-45 Yushima, Bunkyo-ku, Tokyo, 113–8519, Japan. E-mail: yshinoda.phy1@med.tmd.ac.jp

Received 23 December 1998; Revised 2 March 1999; Accepted 16 March 1999

gen and Voogd, 1977; Voogd et al., 1996). Some mossy fiber projections also seem to show longitudinal organization in the vestibulofloccular system (Sato et al., 1983) and the spinocerebellar system (Oscarsson, 1976). However, the somatotopical map of the face established by detailed electrophysiologic investigation does not seem to consist of longitudinal zones, but rather of a mosaic of small patchy areas in the mossy fiber projection from the facial area to the hemispheric ansiform lobule (Shambes et al., 1978). Thus, whether or not there is a common principle in the cortical organization of the projections of different mossy fiber systems remains unclear.

Mossy and climbing fiber projections to the deep cerebellar nuclei (DCN) have not been fully investigated, compared with their projection to the Cx. Determining the existence or nonexistence of excitatory inputs to the DCN from the brainstem is important for our understanding of cerebellar function (Shinoda et al., 1993, 1997). It has been generally assumed that excitatory inputs to the DCN are supplied through collaterals of mossy and climbing fiber afferents to the Cx (Eccles et al., 1967; Ito, 1984). Despite a wealth of anatomic reports on the afferent pathways to the Cx, until recently there have been far fewer studies on afferent projections to the DCN. By using modern reliable anatomic staining methods, the projections from the pontine nucleus, nucleus reticularis tegmenti pontis, IO, and spinal cord to the DCN have been definitely confirmed (Gerrits and Voogd, 1987; Van der Want et al., 1989; Shinoda et al., 1992; Mihailoff, 1993; Matsushita and Yaginuma, 1995). The existence of collateral projection of mossy fibers of the pontine nucleus and the nucleus reticularis tegmenti pontis to the DCN was demonstrated by intra-axonal staining with HRP (Shinoda et al., 1992, 1997), and the collateral projection of climbing fibers to the DCN was identified by labeling single axons with biotinylated dextran amine (BDA) (Sugihara et al., 1996). However, questions still remain as to whether there exist some fibers that project only to the DCN without projecting to the Cx and how many percentages of mossy fibers have axon collaterals to the DCN in different mossy fiber systems.

The lateral reticular nucleus (LRN) is a major mossy fiber source in the medulla. The LRN receives afferents mainly from the spinal cord bilaterally (Oscarsson and Rosén, 1966; Bruckmoser et al., 1970; Künzle, 1973; Clendenin et al., 1974c,d; Ekerot and Oscarsson, 1975) and, additionally, from several supraspinal structures, including the cerebral cortex (Bruckmoser et al., 1970; Ruigrok and Cella, 1995). Now, it is generally accepted that the LRN projects to the bilateral cerebellar cortices with ipsilateral predominance (Matsushita and Ikeda, 1976: Voogd, 1964), and to the "classical spinal receiving area," i.e., the anterior lobe and paramedian lobule, rather than the whole Cx (Clendenin et al., 1974a; Ruigrok and Cella, 1995). Innervations from the LRN to the DCN (Parenti et al., 1996) and to the vestibular nuclei (VN) (Ruigrok et al., 1995) are also bilateral with ipsilateral predominance. The cerebellar cortical projection of the LRN shows a multiple longitudinal zonal pattern (Künzle, 1975; Chan-Palay et al., 1977) that is roughly related to zebrin-identified Purkinje cell zones (Ruigrok and Cella, 1995). These anatomic studies have used an anterograde staining method to examine LRN projection to the Cx, but dealt with mass projection. Information on the entire axon trajectory of the single mossy fibers should reveal us the spatial innervation pattern in the Cx, the frequency of occurrence of nuclear collaterals, and the general topographical correspondence between LRN-cortical and LRN-nuclear projections of the single mossy fibers.

The present study was aimed at revealing characteristic branching patterns of single mossy fibers in the Cx and the DCN by reconstructing the entire trajectory of single axons labeled after the injection of BDA into the LRN in the rat. The results show that single LRN axons give rise to multiple collaterals to the Cx and DCN mainly bilaterally, and these collaterals of single axons appear to make up multiple longitudinal zones that are arranged in a mediolateral direction in multiple lobules.

MATERIALS AND METHODS

Eighteen adult Long-Evans rats of both sexes, weighing between 250 and 310 g, were used in the present study. Fifteen of them received injections of BDA in the LRN, one in the central cervical nucleus (CCN) and two in the lateral medulla and inferior cerebellar peduncle (icp). The surgery and animal care conformed to The Principles of Laboratory Animal Care (NIH publication No. 85–23, revised in 1985) and also to Guiding Principles for the Care and Use of

Abbreviations

I–X	lobules I–X
AMB	nucleus ambiguus
BDA	Biotinylated dextran amine
C	caudal
CCN	central cervical nucleus
COP	copula pyramidis
Crus I	crus I ansiform lobule
Crus II	crus II ansiform lobule
Cx	cerebellar cortex
D	dorsal
DCN	deep cerebellar nuclei
DN	dentate nucleus
FL	flocculus
FN	fastigial nucleus
icp	inferior cerebellar peduncle
IO	inferior olive nucleus
IP	interposed nucleus
IPa	anterior interposed nucleus
IPp	posterior interposed nucleus
LVN	lateral vestibular nucleus
LRN	lateral reticular nucleus
LRNm	the magnocellular part of the LRN
LRNp	the parvicellular part of the LRN
LRNst	the subtrigeminal part of the LRN
Lt	left
MVN	medial vestibular nucleus
PGRNI	paragigantocellular nucleus
PHA-L	*Phaseolus vulgaris* leucoagglutinin
PFL	paraflocculus
PM	paramedian lobule
R	rostral
Rt	right
scp	superior cerebellar peduncle
SCT	spinocerebellar tract
Sim	simple lobule
SPV	spinal trigeminal nucleus
SVN	superior vestibular nucleus
V	ventral
VN	vestibular nucleus

Animals in the Field of Physiological Sciences (The Physiological Society of Japan, 1988).

Surgical procedures and tracer application

The animals were anesthetized with an intraperitoneal injection of ketamine (130 mg/kg body weight), xylazine (Rompun, Bayer, Germany; 8 mg/kg), and atropine (0.4 mg/kg) and placed in a stereotaxic apparatus. Heart rate and rectal temperature were monitored continuously. Supplemental doses of ketamine (13 mg/kg) and xylazine (1 mg/kg) were given every 30 minutes starting 1 hour after the initial dose, as required. A heating pad was used to keep the rectal temperature between 35 and 37°C. After incision of the dorsal neck skin, a cut was made in the ligament between the skull and the first vertebra.

BDA (D-1956, 10,000 MW, Molecular Probes, Eugene, OR) was dissolved in physiologic saline to give a concentration of 10–15%. A glass micropipette (tip diameter, 4 μm) was filled with this solution. The coordinate of the insertion point for the LRN was approximately 0.5 mm caudal from the caudal edge of the area postrema, 1.8 mm lateral to the midline. The pipette was tilted 20° caudally in the parasagittal plane, and inserted to a depth of about 3.5 mm from the surface. Neural activity was monitored from the pipette to facilitate locating the LRN. A small injection was made either with pressure (about 0.1 μl) or electrophoresis (2μA positive current pulses of 1-second duration at 0.5 Hz for 30 minutes). Pipettes were left in situ for 5 minutes after injection before they were withdrawn. The wound was cleaned with povidone-iodine, and an antibiotic (cefmetazole) was applied to the wound before suturing.

Fixation and histochemistry

After a survival period of 6 to 8 days, the animals were deeply anesthetized with ketamine (150 mg/kg) and xylazine (12 mg/kg) and perfused through the ascending aorta. Chilled perfusate containing 0.8% NaCl, 0.8% sucrose, and 0.4% glucose in 0.05 M phosphate buffer (pH 7.4, about 4°C, and about 400 ml) was given and followed by a fixative containing 2% paraformaldehyde, 0.6% glutaraldehyde, and 4% sucrose in 0.05 M sodium phosphate buffer (pH 7.4, about 4°C, and about 500 ml) delivered over 30 minutes. Dissected brains (cerebellum and medulla oblongata) were kept in the same fixative overnight at 4°C and then in 30% sucrose in phosphate buffer (0.05 M, pH 7.4, 4°C) for 1–2 days. The brain was then embedded in a gelatin block.

Serial coronal sections 35- or 50-μm thick were cut on a freezing microtome. Sections were treated with biotinylated HRP-avidin complex (Standard ABC kit KT-4000, Vector, Burlingame, CA), and a cobalt-glucose oxidase method (Itoh et al., 1979; Sugihara et al., 1996) was used for the diaminobenzidine reaction. The sections were then mounted on chrome alum–gelatinized slides, dried overnight, and cover-slipped with Permount. After reconstruction of labeled axons, some of the sections were counterstained with thionin.

Light microscopic reconstruction

Drawings of labeled axons and terminals were made at an objective magnification of ×2 to ×60, with the aid of a Nikon microscope equipped with a camera lucida apparatus. Trajectories of single-labeled axons were reconstructed on serial sections by connecting cut ends of an axon on one section to the corresponding cut ends of the same axon on the successive sections as was done with the intra-axonal injection of HRP (Futami et al., 1979; Shinoda et al., 1981, 1986, 1992). Reconstructions in the coronal plane were sometimes converted to those in the parasagittal plane, by measuring depths and replotted.

In drawings of camera lucida images, the fibers and swellings were drawn thicker than scale for clarity, as is conventionally done in drawings of reconstructed fibers. The cerebellar lobules were defined according to Larsell (1952) and Voogd (1995). Subdivisions of the cerebellar and vestibular nuclei were determined according to the descriptions of Korneliussen (1968), Voogd (1995), and Rubertone et al. (1995). The nomenclature used generally followed Swanson (1992) and Voogd (1995). Some photomicrographs were obtained with a computer-aided dynamic focusing system (MCID image analysis system, Imaging Research, Inc., St. Catharines, Ontario, Canada).

RESULTS

Injection sites

The LRN is conventionally separated into (1) a ventrolateral small parvicellular division (LRNp), (2) a dorsal and lateral large magnocellular division (LRNm), and (3) a small subtrigeminal division at the very rostral position (LRNst) (Brodal, 1943; Walberg, 1952). Each injection site in this study is schematically summarized in representative transverse sections at 250-μm intervals (Fig. 1). In 14 experiments, injections of BDA were localized in the LRNm (n = 10), in the LRNm with slight spread into the LRNp (n = 3), and in the LRNp (n = 1).

During the reconstruction of single axonal trajectories on serial sections, we noticed that some labeled axons in the cerebellum could be traced through the injection sites in the LRN as far as the spinal cord. This finding suggested that injection of BDA into the LRN might label passing fibers of spinocerebellar tract (SCT) neurons (Matsushita and Ikeda, 1976). In fact, in some experiments in which many passing fibers running caudally from the LRN were labeled, several retrogradely labeled cells were found in the CCN in the upper cervical spinal cord. Based on an electrophysiologic study some SCT axons have been suggested to send collaterals to the LRN (Alstermark et al., 1990). These findings indicated that BDA injection into the LRN could label SCT axons by either uptake from passing fibers or retrograde uptake from axon collaterals. Therefore, it was essential to differentiate labeled LRN axons from SCT axons before analyzing the morphology of labeled axons originating from the LRN.

LRN projection distinguished from SCT projection

Among all of the reconstructed labeled axons (n = 44), eight could be traced down to their cell bodies in the LRN. This tracing was possible when a cell body and its axon were not in the very center of the injection site, which was too darkly labeled to distinguish cellular components. Another 21 axons were identified as LRN axons (see below), although their cell bodies could not be identified. On the other hand, 15 other axons could be followed through or near the LRN and further down to the spinal cord, indicating that they belonged to SCT neurons. In coronal sections of the central medulla, the icp occupied the white matter underneath the lateral surface of the

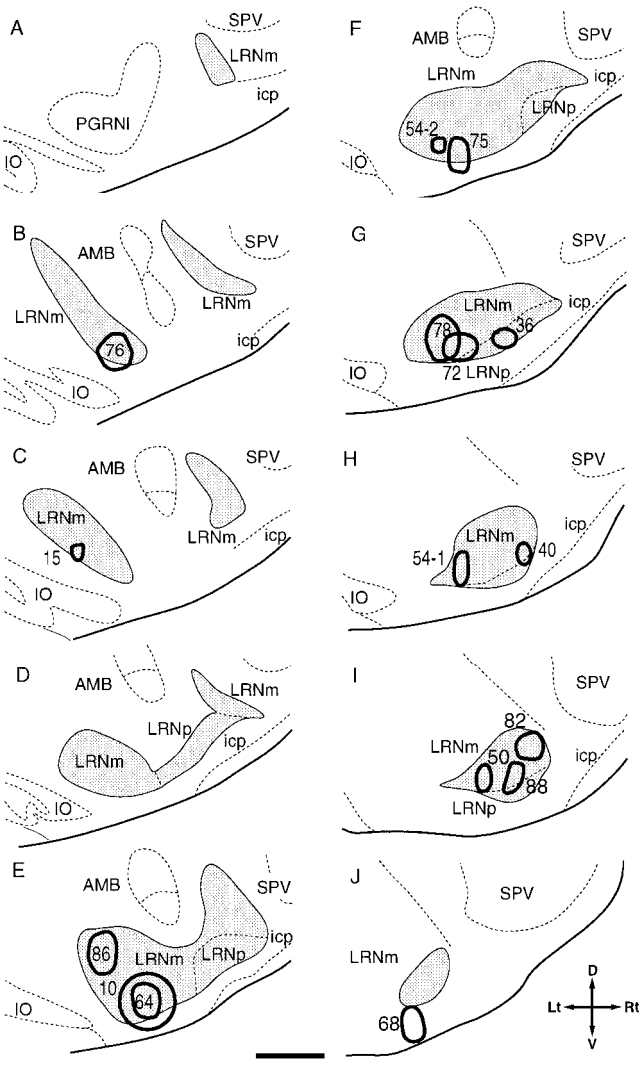

Fig. 1. Injection sites of biotinylated dextran amine (BDA) in the lateral reticular nucleus (LRN) mapped in representative transverse sections of the right ventral medulla. Sections are 250µm apart and ordered from the rostral to the caudal level (**A–J**). Injections 68, 50, 54, 64, 72, 75, and 76 were made on the left side, but plotted on the right side symmetrical to the midline. For abbreviations, see list. Scale bar = 0.5 mm.

medulla covering from its dorsolateral to ventrolateral portion. Although the dorsolateral part of the icp contained labeled axons running longitudinally, which directly entered the cerebellum (shaded areas in Fig. 2A,C,E), the lateral and ventrolateral part of the icp contained axons that ran mainly along the lateral surface of the medulla in the transverse plane. When axons running through the lateral part reached the dorsolateral part, they changed directions and ran longitudinally (Fig. 2H). In the coronal sections at the level of the most rostral IO, a fiber bundle originating from the LRN was already in the dorsolateral part of the icp (shaded area in Fig. 2A,C). All of the axons that were identified as LRN axons by tracing down to their somata were located within this bundle. The number of axons that were not within the dorsolateral part of the icp seemed to vary depending on BDA injection sites into the LRN (Fig. 2A,B and C,D). None of the axons that were identified as SCT axons were involved in the dorsolateral part of the icp at the level of the LRN. We considered that labeled axons that were not within the dorsolateral icp were not LRN axons.

To further confirm the difference in the pathways between LRN axons and SCT axons, the trajectories of labeled SCT axons were traced in the spinal cord, medulla, and cerebellum after BDA injection into the CCN in the spinal cord. Figure 2H summarizes the trajectories of four fiber bundles in the parasagittal plane. The two fiber bundles (filled and open arrowheads) are the main fiber bundles labeled after BDA injections into the caudal and rostral LRN, respectively. Both bundles included some axons that could be traced down to their somata. The other two bundles (open and filled arrows) were fibers from the CCN (Fig. 2G), which could be regarded as representing two main paths of SCT axons; one path through the superior cerebellar peduncle (open arrow) corresponding mainly to the ventral and rostral SCTs, and the other path through the icp (filled arrow) corresponding mainly to the dorsal SCT (Matsushita and Yaginuma, 1995). In contrast to Figure 2B, no cerebellar projecting axons were seen to ascend to the lateral medullary white matter in the dorsal direction at the level of the LRN (Fig. 2F). All of the labeled axons were in the lateral and ventrolateral parts of the icp (caudal SCT bundle) or in the ventral medulla (rostral SCT bundle) at the level of the most rostral IO (Fig. 2E) on bilateral sides. In addition, many axon terminals were observed within the LRN (predominantly ipsilateral) (not shown), suggesting that they projected to the LRN by means of collaterals, which could partly explain why SCT axons were easily labeled by BDA injection in the LRN. The reconstructed fiber bundles shown in Figure 2H indicate that LRN axons enter the dorsolateral part of the icp at a more caudal level than the caudal bundle of SCT axons. Based on these criteria, we regarded 21 reconstructed axons as LRN axons, because they ran through the dorsolateral white matter at the level of the rostral end of the IO. They could be traced proximally to the injection sites within the LRN, and none of them passed out through the LRN.

We were able to estimate the numbers of labeled LRN axons and SCT axons separately in each experiment. In the coronal sections at the level of the rostral-most IO, LRN axons ran in the dorsolateral part of the icp, whereas SCT axons in the caudal bundle were in the ventrolateral white matter. In the coronal sections about 1 mm rostral to the rostral end of the DCN, SCT axons in the rostral bundle ran caudally in the dorsal brainstem.

General observations

Axonal tracing and terminal mapping were done in 11 experiments (exp 36, 40, 50, 54, 64, 72, 76, 78, 82, 86, and 88 in Fig. 1) in which BDA injections were localized within the LRN. The diameter of the tracer spread at the injection site was about 100 to 300 µm (223 ± 77µm, mean ± S.D.). The number of labeled LRN axons ranged from 6 to 90 (29.5 ± 24.0, n = 11), and that of labeled SCT axons ranged from 1 to 34 (10.6 ± 10.1). The fraction of SCT axons among all labeled axons projecting to the cerebellum ranged from 0.13 to 0.33 (0.24 ± 0.07). However, these values are probably an overestimate of the true involvement of SCT axon terminals among LRN axon terminals in the Cx, because even stem axons of most SCT axons were so faintly labeled in the brainstem that their distal branches

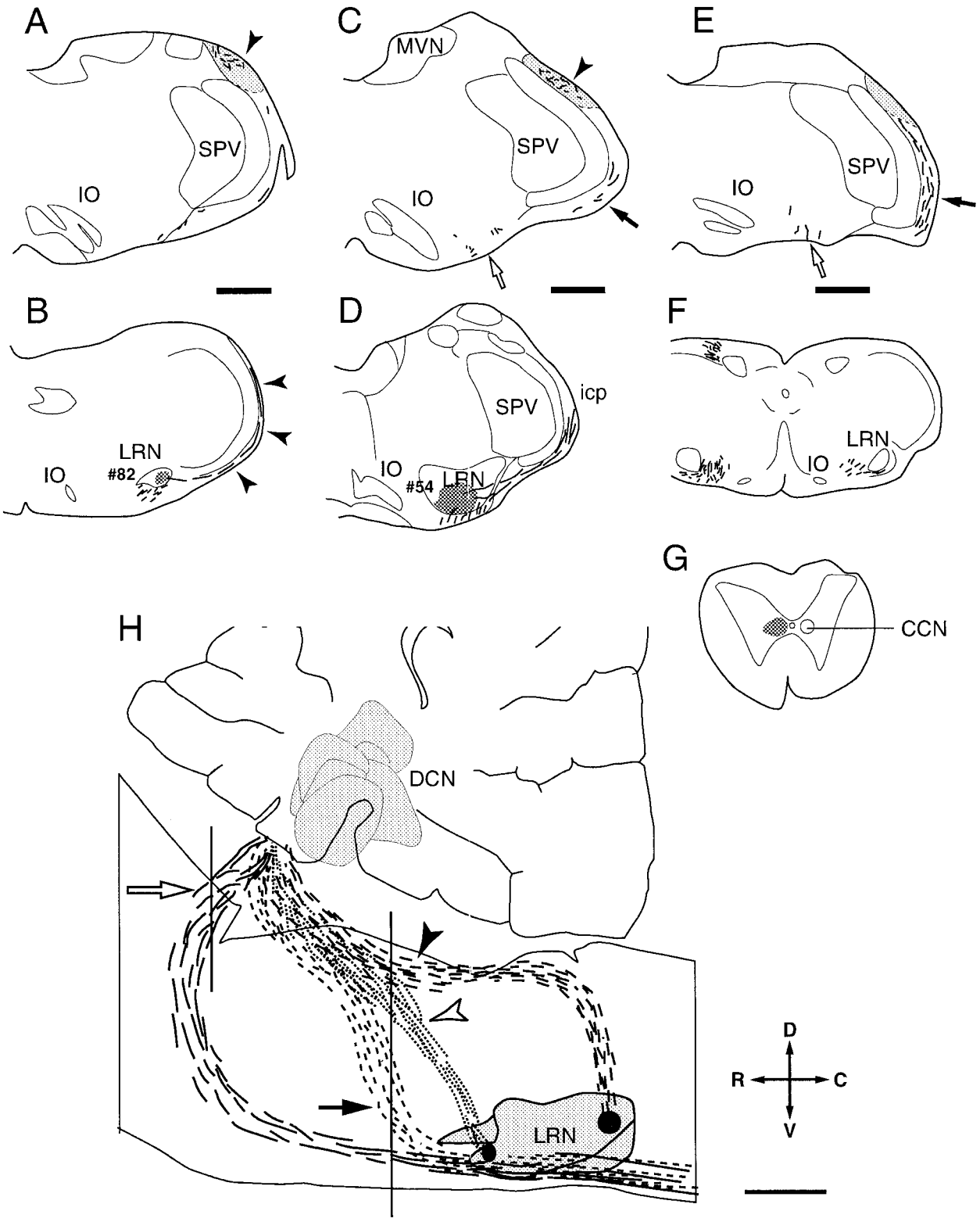

Fig. 2. Separation of lateral reticular nucleus (LRN) axons and spinocerebellar tract (SCT) axons in the medullary white matter. **A,B:** Camera lucida drawings in a transverse plane showing axons at the level of the rostral IO (A) labeled by an injection of biotinylated dextran amine (BDA) into the caudal LRN at the level of the caudal-most IO (B). Filled arrowheads indicate labeled LRN axons. **C,D:** Drawings of labeled axons at the level of the rostral IO (C) after injection of BDA into the central LRN at the level of the caudal IO (D). Some SCT axons (filled and open arrows) were also labeled in the ventrolateral white matter of the medulla. Filled arrowhead indicates labeled LRN axons. **E–G:** Camera lucida drawings of SCT axons at the level of the rostral and caudal poles of the IO (E,F), which were labeled by an injection of BDA into the central cervical nucleus (CCN) at C4 (G). An open arrow shows BDA-labeled fibers that do not enter the icp but run more rostrally at the medulla, whereas a filled arrow shows BDA-labeled CCN fibers running through the icp. **H:** Reconstructed trajectories of bundles of axons from injection sites in the caudal LRN (filled arrowhead) and rostral LRN (open arrowhead), and of rostral and caudal bundles (open and filled arrows, respectively) of SCT axons labeled by an injection into the CCN. The two vertical straight lines indicate the level of the rostral pole of the IO and the level 1 mm rostral to the cerebellar nuclei, in which the number of labeled axons that belonged to each bundle of SCT and LRN axons could be counted separately. Shaded areas in A, C and E indicate a dorsolateral portion of the inferior cerebellar peduncle in which fibers ran longitudinally toward the entrance to the cerebellum. Shaded areas in B, D, and G indicate injection sites of BDA. For abbreviations, see list. Scale bars = 1 mm.

in the cerebellar white matter became untraceable. Therefore, despite the contamination by labeled SCT axons in the cerebellar peduncles, contamination by the terminals of these SCT axons among LRN axon terminals may be much less than is indicated by these numbers.

All of the labeled fibers in the Cx bore rosette-type terminals characteristic of mossy fibers (Ramón y Cajal et al., 1911). No climbing fibers or axons of other types bearing only small non–rosette-type swellings were observed. Therefore, virtually all of the LRN axons projecting to the Cx appeared to take the form of a mossy fiber. We extensively analyzed the data from four experiments (exp 40, 76, 82, and 88) in which the fraction of labeled SCT axons was relatively small (23%, 23%, 13%, 25%, respectively) on terminal distributions in the Cx, DCN, and VN. Abundant labeled fibers of very small diameters bearing small swellings were observed in the DCN and VN as in the Cx. They were presumably collateral terminations of LRN axons, as shown by single axon tracings in later sections.

Observations from serial coronal sections showed some differences in the distribution of labeled terminals in the Cx, DCN, and VN in these four experiments. However, these four cases had many common characteristic features of the distribution pattern of axon terminals of the LRN projection in the cerebellum and were representative of all of the 14 experiments. Figure 3 shows a typical example of the distribution of axon terminals in the Cx after BDA injection into the rostral part of the LRNm (exp 76). Rosettes were densely distributed in the Cx in the bilateral vermis and intermediate areas and hemispheres of lobules II, III, IV, and V (most dense in IV and V). A less-dense distribution was seen in the bilateral vermis of lobules VI, VII, VIII, and IX, and in hemispheres of simple and ansiform lobules, and copula pyramidis. A small number of rosettes were seen in the left paramedian lobule, and no rosettes were seen in the flocculus, paraflocculus, or nodulus. There were slightly more rosettes on the ipsilateral side (n = 3,836) than on the contralateral side (n = 2,722), and the ratio of ipsilateral terminals to contralateral terminals in the Cx was 1.41:1. Because BDA was injected into the left LRN, this finding indicated slight ipsilateral predominance. In this distribution (Fig. 3), multiple zones of clusters of rosettes were obvious in the vermis of lobules III, V, and VI, and weak zones seemed to be present in other areas such as lobules IV and VII. In lobules III, V, and VI, three zones with a dense distribution of rosettes were seen, and the width of each was about 0.5 mm. One of the zones in the vermis was located at the midline, and the other lateral zones were located about 0.6 mm (lobule III) or 1.2 mm (lobule V, VI) from the midline bilaterally. Swellings in the DCN and VN in the same experiment were distributed mainly in the fastigial (FN), anterior interposed (IPa), posterior interposed (IPp) and dentate (DN) nuclei, and the lateral vestibular nuclei (LVN) bilaterally (Fig. 4). Dense distribution was seen in the ventromedial part of the IPp, the medial part of the IPa, the ventrolateral part of the FN and the dorsal LVN bilaterally.

In one experiment (exp 82 in Fig. 1), axon terminals were distributed almost exclusively ipsilaterally in the Cx (Fig. 5) and mainly ipsilaterally with some contralateral distribution in the DCN (Fig. 6). This injection site was in the dorsolateral part of the caudal LRNm. Rosettes were distributed in lobules II, III, IV, and V in the anterior lobe, and in lobules VI, VII, VII, and IX, and in the simple, ansiform, and paramedian lobules and copula pyramidis only ipsilaterally in the posterior lobe. A small number of rosettes were seen in lobule I and the ansiform lobule. No rosettes were seen in the flocculus, paraflocculus or nodulus. Dense distributions were seen in the junction of the lateral-most vermis and the intermediate area of lobules IV and V, in the lateral-most hemisphere of lobule II, III, IV, and V, in the junction of the lateral vermis and intermediate area in lobule VI-simple lobule, lobule VII-paramedian lobule, and lobule VIII-copula pyramidis, and in the hemispheric portion in the paramedian lobule and copula pyramidis (most dense in lobule V). Areas of dense distribution seemed to be arranged in a multiple zonal pattern in the anterior lobe and in the paramedian lobule and copula pyramidis. In the anterior lobe, a zone about 0.5 mm wide could be recognized in the right vermis about 1 mm lateral from the midline. The second zone was about 1 mm or more wide and was located in the lateral-most vermis through the intermediate area. The third zone was about 1 mm wide and was located in the lateral-most hemisphere. In the paramedian lobule and copula pyramidis, four zones about 0.5 mm wide seemed to be located in semiparasagittal planes separated by about 1 mm from the junction between the vermis and intermediate area to the lateral-most hemisphere. In the DCN and VN of this experiment, the distribution of labeled terminals was predominantly ipsilateral as in the Cx (Fig. 6). A dense distribution of swellings was seen in the medial part of the ipsilateral IP, and a small number of swellings were seen in bilateral FNs and ipsilateral DN. However, swellings were almost negligible in the contralateral DN and the contralateral lateral IP. In the VN, a dense distribution of swellings was seen in the dorsal part of the ipsilateral LVN but no terminals were seen in the contralateral VN.

In the other two cases of mapping in which the BDA injection was located in the caudolateral LRNm (exp 40) and caudoventral LRNm (exp 88), the distribution of labeled terminals was similar to that with injection into the rostral LRNm (exp 76 plotted in Figs. 3, 4). In experiments in which detailed mappings were not made (7 of 11 experiments), the distribution of terminals in the Cx, DCN, and VN was roughly similar to the case shown in Figures 3 and 4. In summary, LRN axons originating from the LRNm generally showed a bilateral projection with ipsilateral predominance in the anterior lobe and some areas, including the paramedian lobule and copula pyramidis, in the posterior lobe with a multiple longitudinal zonal pattern. However, axons originating from the dorsolateral part of the caudal LRN showed a virtually exclusive ipsilateral projection.

General morphology of single reconstructed LRN axons

The entire trajectories of single LRN axons could be completely reconstructed from the injection site to terminations of every branch in 11 identified LRN axons. In addition, nearly complete reconstruction, except for distal portions of some branches in the cerebellum, was possible in 18 identified LRN axons. These axons (n = 29) were used for a detailed morphologic analysis, and other partially reconstructed axons (n = 69) were used to supplement the data.

Among the 11 completely reconstructed axons, the cell bodies were identified in two cases. The long and short

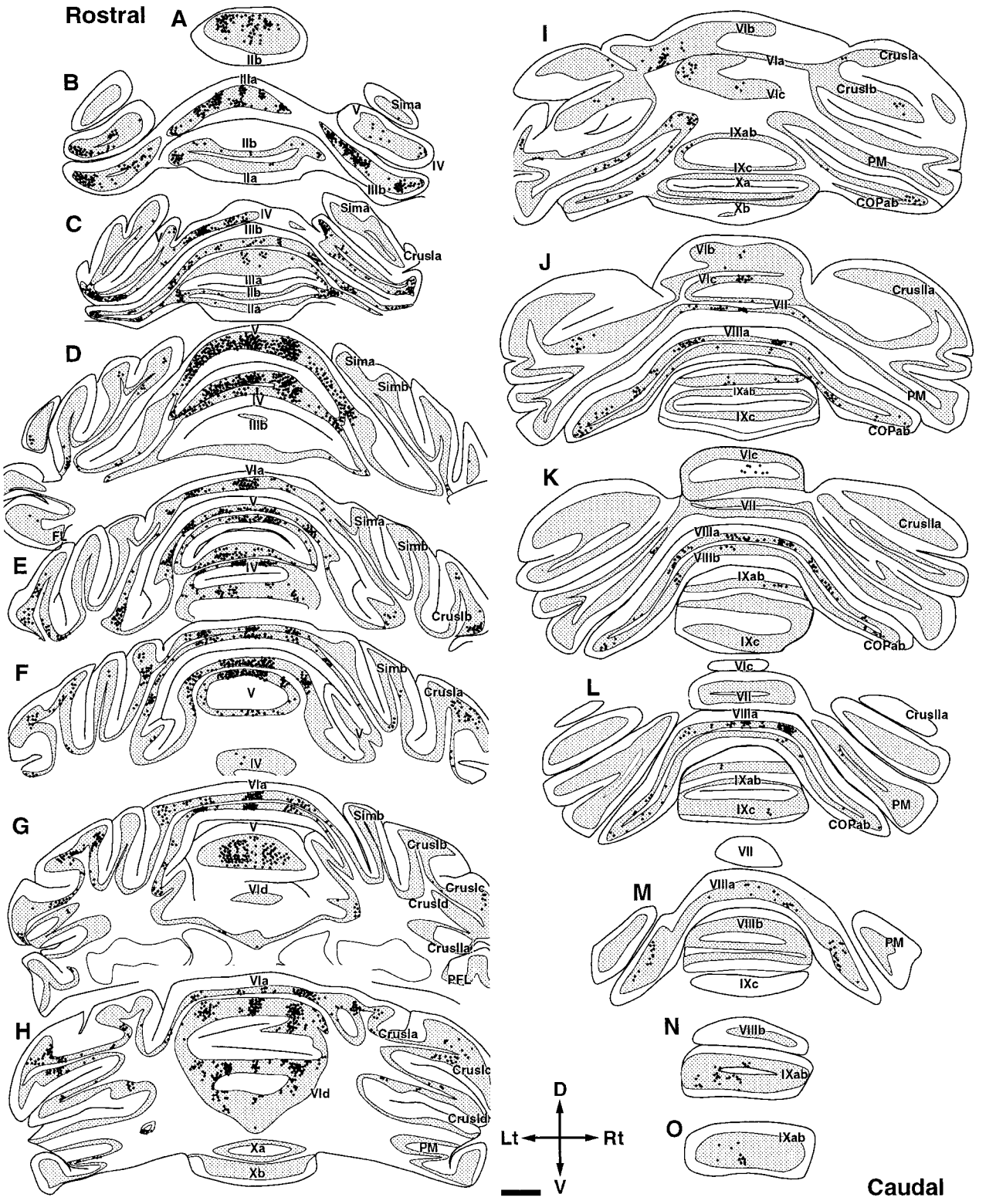

Fig. 3. Mapping of mossy fiber rosettes in the cerebellar cortex (Cx) after biotinylated dextran amine injection into the rostral part of the left lateral reticular nucleus (LRN) (exp 76), showing bilateral projection with ipsilateral predominance and zone-like terminal distribution in the Cx. Each dot represents a single rosette-type bouton. All terminals that were labeled in five consecutive 50-μm-thick sections were plotted on individual representative transverse sections that are separated from each other by 250 μm (**A–O**, rostral to caudal). Roman numbers indicate names of lobules. For abbreviations, see list. Scale bar = 1 mm.

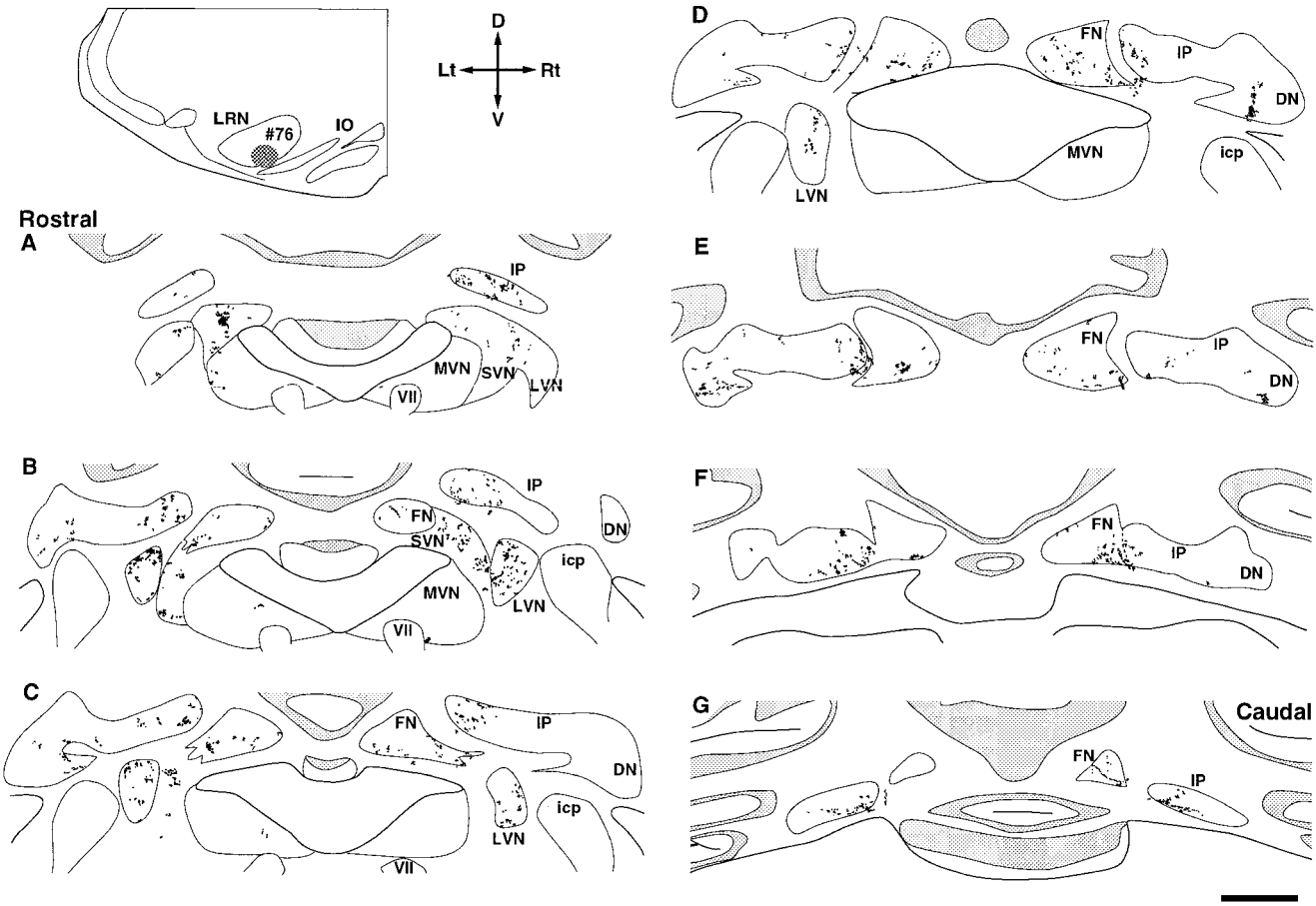

Fig. 4. Distribution of axon terminals in the cerebellar and vestibular nuclei after biotinylated dextran amine injection into the rostral part of the left LRN (injection site in the upper left **inset**). The same material as in Figure 3. Each dot represents a single terminal swelling. All of the swellings obtained from five consecutive 50-µm-thick sections were plotted on representative frontal sections that were separated from each other at 250-µm intervals (**A–G**, rostral to caudal). For abbreviations, see list. Scale bar = 1 mm in G (applies to A–G).

diameters of the identified cells were 26 and 16µm (fiber 6, exp 82), and 26 and 13µm (fiber 10, exp 88), respectively (Fig. 7B). These neurons were large LRN neurons according to Walberg's (1952) drawing and the classification by Kapogianis et al. (1982). In 18 semicompletely reconstructed LRN axons, the cell bodies were identified in four cases, and the long diameter ranged from 8 to 29 µm, whereas the short diameter ranged from 8 to 9 µm, indicating that these axons were from both small and large neurons. Axons from large and small cerebellar-projecting LRN neurons ran through a similar path to the cerebellum and made mossy fiber terminations. However, a detailed comparison of the branching patterns of large and small neurons could not be made because axons originating from small neurons could not be completely reconstructed in the present study.

Most of the reconstructed axons of LRN neurons passed through the ipsilateral icp to the cerebellum (n = 25 of 29; group 1A and 1B in Table 1; Figs. 9, 10, 11). These axons originating from the LRN ran laterally and entered the ventrolateral part of the icp under the lateral surface of the medulla. The axons then ran in the dorsorostral direction, entered the dorsolateral part of the icp, and made a turn rostrally toward the cerebellum. Some of the reconstructed LRN axons (n = 4 of 29; group 2A and 2B in Table 1; Fig. 8) ran medially through or under the ipsilateral IO, passed the midline, ran through or under the contralateral IO, and entered the ventrolateral part of the contralateral icp. These axons entered the cerebellum through the contralateral icp. Except for the laterality in the icp, these axons followed a path similar to that of the other LRN axons.

To estimate the relative numbers of LRN neurons that sent their axons through the ipsilateral and contralateral icp, larger volumes of BDA (4–5 µl) were injected with pressure in the lateral medulla, including the icp in two experiments, and the number of retrogradely labeled neurons was counted in the bilateral LRN. Labeled cells were more abundant in the ipsilateral LRN (n = 1,137, 1,043) than in the contralateral LRN (n = 102, 114), indicating that about 90% of the LRN neurons projecting to the cerebellum sent their axons through the ipsilateral icp.

Stem axons passed through the icp without any branches in the medulla and entered the cerebellar white matter rostral to the DCN. Generally, an arbor of an LRN axon within the cerebellum could be regarded as consisting of a thick stem axon running transversely, cortical branches of

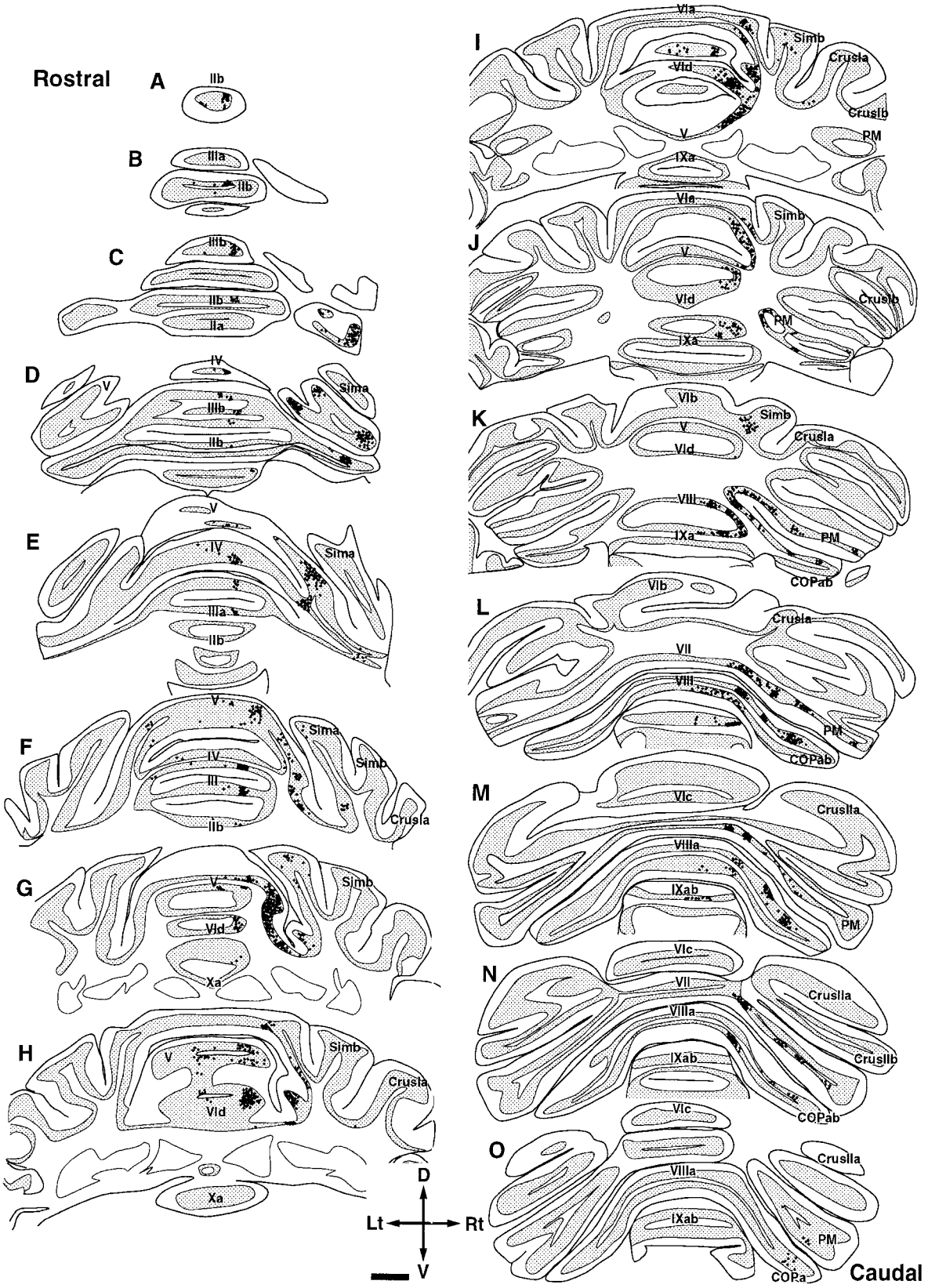

Fig. 5. Mapping of mossy fiber rosettes in the Cx after biotinylated dextran amine injection into the dorsocaudal part of the right LRN (exp 82). All terminals that were labeled in five consecutive 35-µm-thick sections were plotted on individual representative transverse sections which are separated from each other by 175µm (**A–O**, rostral to caudal). No terminals were seen in sections caudal to section O. Note the predominant ipsilateral projection and multiple longitudinal zonal arrangement in the right copula pyramidis and paramedian lobule. Refer to Figure 3 for the format. For abbreviations, see list. Scale bar = 1 mm.

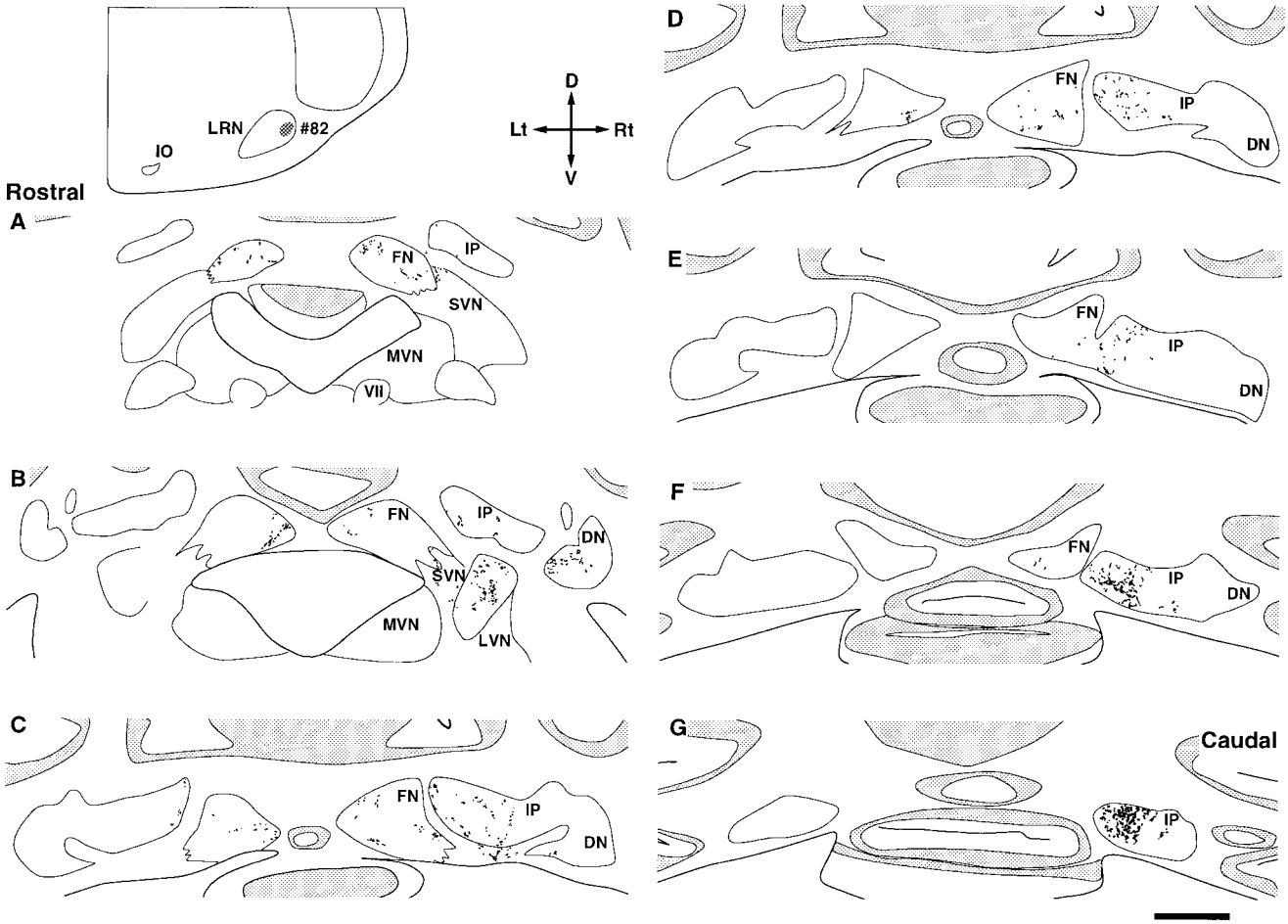

Fig. 6. **A–G:** Mapping of axon terminals in the cerebellar and vestibular nuclei in the same experiment as in Figure 5 (injection site shown in the upper left **inset**). Predominant ipsilateral projection was seen. Refer to Figure 4 for the format. For abbreviations, see list. Scale bar = 1 mm in G (applies to A–G).

various diameters, and very thin nuclear branches. The stem axons ran medially toward the midline in the deep white matter rostral and dorsal to the DCN. Some stem axons did not cross the midline in the cerebellum and made projections nearly exclusively on the same side as the icp through which they passed (n = 4 of 29; groups 1A and 2A in Table 1). The other stem axons (n = 25 of 29; group 1B and 2B in Table 1) crossed the midline within the cerebellum to make bilateral projections. Thus, LRN axons could be divided into four groups in terms of the laterality of the icp that they passed through relative to their cell bodies, and by their projection to either the unilateral or bilateral cortices. All of the completely reconstructed axons had more terminals in the Cx on the same side as the icp through which they ran (Table 1). However, as will be described later, there were some differences among individual axons concerning the laterality of their projections in the Cx and DCN, the number of primary collaterals, their projection lobules, and the morphology of collaterals in the DCN. We tentatively divided LRN axons into four groups; group 1 (n = 25) contained LRN neurons with stem axons that passed through the ipsilateral icp, and group 2 (n = 4) contained those with stem axons through the contralateral icp. These neurons were further divided into groups A and B according to their projection to the unilateral or bilateral cortices. As summarized in Table 1, 3 neurons were in group 1A, 22 were in group 1B, 1 was in group 2A, and 3 were in group 2B.

Although running transversely in the cerebellar white matter toward the contralateral side, stem axons gave rise to several primary collaterals to the Cx and DCN. Individual primary collaterals arose at an almost right angle (Fig. 7C) from the stem axon, and ran largely in a parasagittal plane in the Cx. Primary collaterals projecting to lobules II and III were directed almost horizontally and rostrally, whereas primary collaterals projecting to lobules IV–V were directed rostrodorsally and those projecting to lobules VI or VII were directed dorsally or dorsocaudally. On their way through the Cx, individual primary collaterals widely ramified mainly in a dorsoventral direction, but did not spread so widely in a mediolateral direction, so that each collateral terminated as mossy fiber rosettes in the granular layer in a relatively narrow longitudinal zonal area covering one to four lobules (Figs. 8–11). The number of cortical primary collaterals given off from a transverse stem axon in the deep cerebellar white matter was five to nine (7.0 ± 1.0, n = 29). In each of the bilaterally projecting neurons, the number of ipsilateral

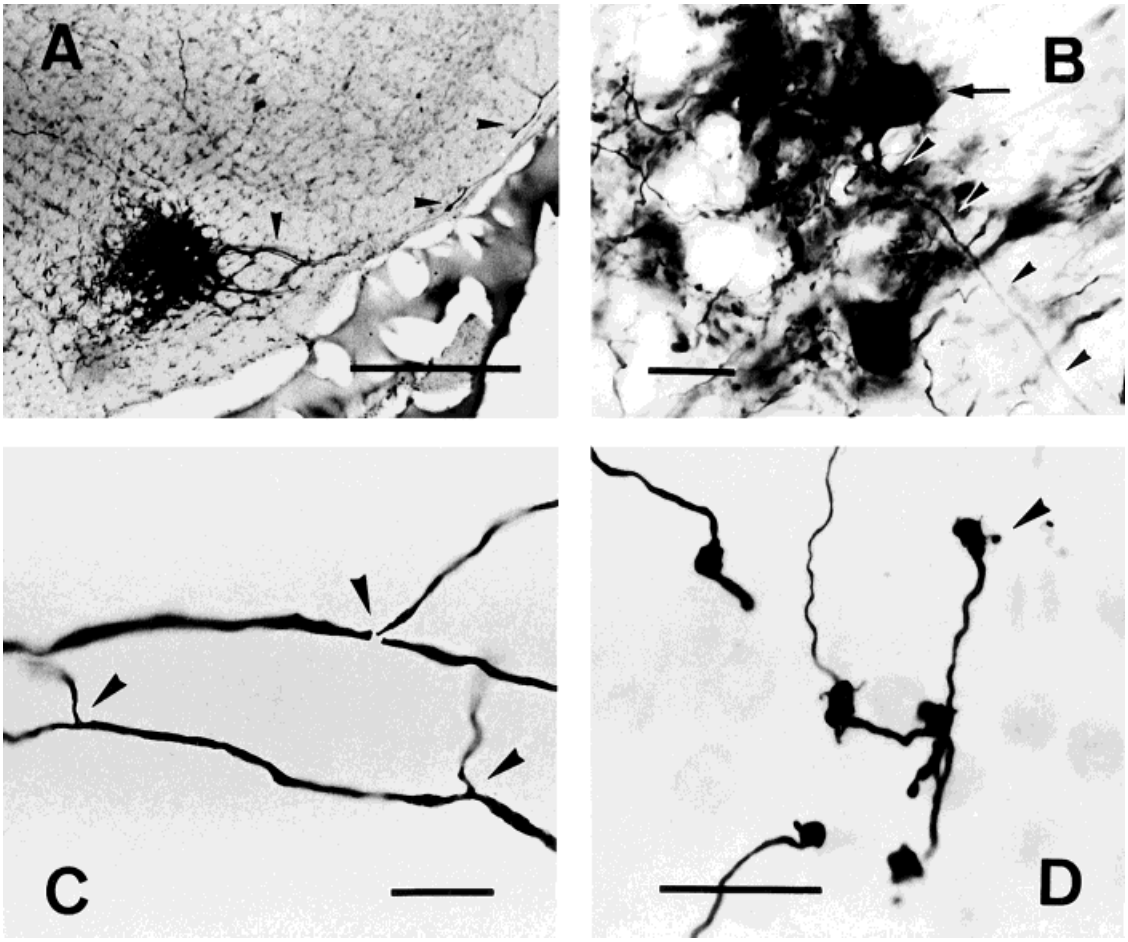

Fig. 7. Photomicrographs of labeled lateral reticular nucleus (LRN) axons and their terminals in the cerebellar cortex Cx). **A:** Injection site in the LRN (exp 82) and axons running laterally and then dorsolaterally out of the injection site and through the inferior cerebellar peduncle (arrowheads). Coronal section of the medulla including the center of the injection site in the right LRN. **B:** Labeled cell body of an LRN neuron (arrow) whose axonal trajectory (arrowheads) was completely reconstructed in the cerebellum. **C:** Primary collaterals arising at an approximately right angle from horizontally running stem axons of LRN neurons in the deep cerebellar white matter. Arrowheads indicate branching points. **D:** Rosettes in the Cx. Arrowhead indicates a small satellite swelling borne on a short branchlet that protruded from a rosette. Scale bars = 0.5 mm in A; 25 μm in B,C; 50 μm in D.

primary collaterals was three to five (3.8 ± 0.8, n = 25), and the number of contralateral primary collaterals was two to six (3.7 ± 1.4, n = 25). In each of the unilateral projecting neurons, the number of primary collaterals was five to eight (6.0 ± 1.2, n = 4). These primary collaterals further ramified to innervate one to four lobules. A single longitudinal arrangement of terminals in the Cx usually originated from a single primary collateral, but occasionally originated from multiple primary collaterals (Figs. 9, 10).

The diameters of the stem axons in the icp ranged from 2.5 to 3.9 μm. After the first branching of a primary cortical collateral, the diameters of the main branches were 1.5–2.0 μm. The diameters of primary collaterals at ramification points ranged from 1.0 to 1.5 μm. The diameters of the stem axons decreased slightly while giving off several primary cortical collaterals. Each cortical collateral made several bifurcations in the white matter and in the granular layer with a slight or insignificant decrease in diameter. Eventually, the diameters of individual mossy fibers in the Cx became 0.6–1.3 μm near their termination sites.

Distribution of terminals of single LRN axons in the cerebellar cortex

Each terminal branch of single LRN axons always terminated as rosette-type terminals (Fig. 7D). The rosette-type terminals borne on the LRN axons had a long diameter of 10.7 ± 2.7 μm (n = 20) and a short diameter of 8.0 ± 1.8 μm (n = 20). They were borne either at the end (terminal type) or in the middle of the fiber (*en passant* type) in the granular layer of the Cx. The number of rosettes per LRN axon ranged from 84 to 219 (154.0 ± 37.0, n = 11) (Table 1). In each of the bilaterally projecting axons, the ratio of axon terminals in the ipsilateral Cx to those in the contralateral Cx ranged from 1.26:1 to 2.26:1 (1.69 ± 0.40, n = 7). Ipsilateral dominance of the LRN projection was recognized even at the level of a single neuron. Occasionally, a thin short branchlet (diameter, about 0.5 μm; length 5–50 μm) protruded from a terminal or *en passant* rosette, and a small round swelling (diameter 1.4 ± 0.3 μm, n = 12) was borne at the end of the thin short branchlet in the granular layer (Fig. 7D, arrowhead).

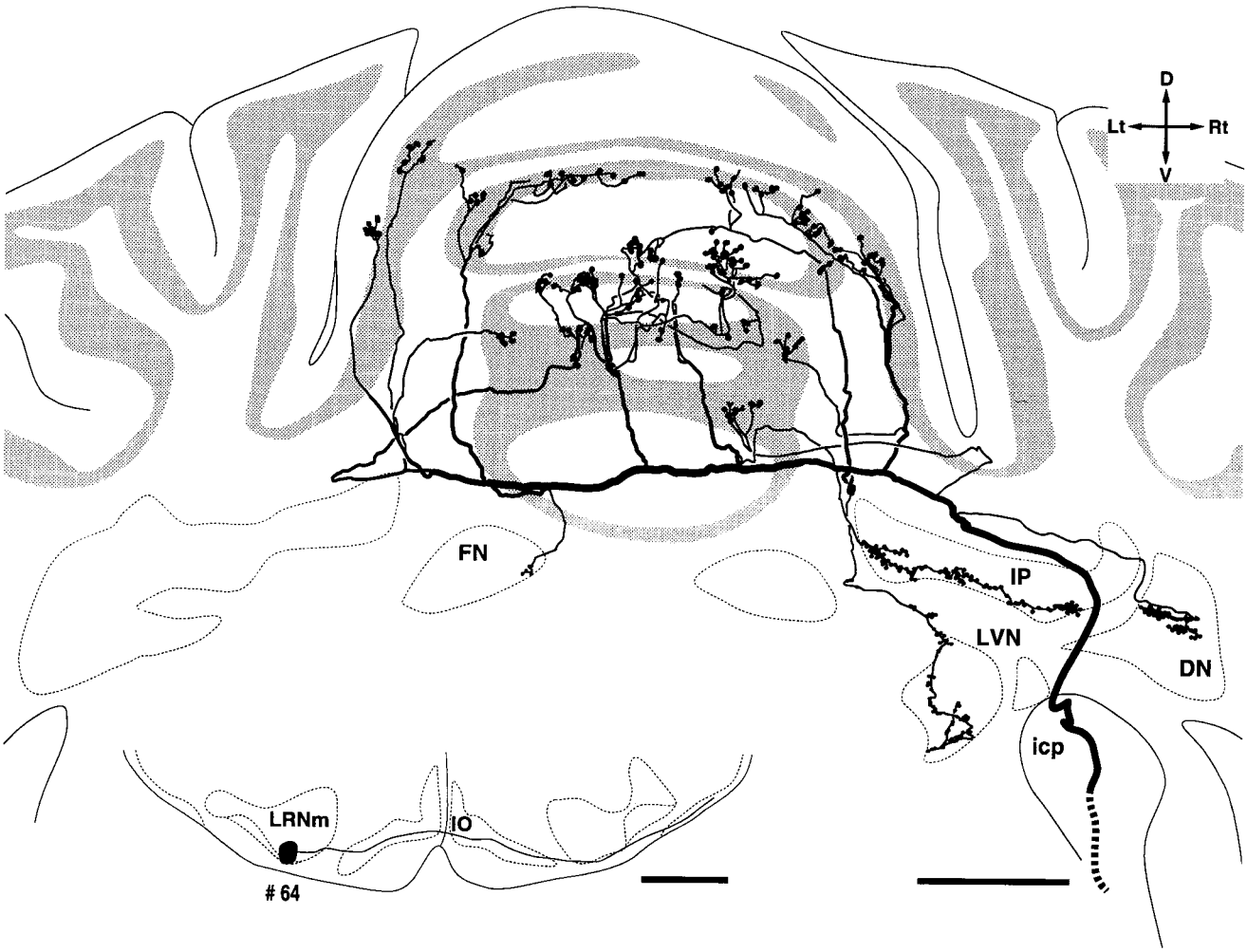

Fig. 8. Frontal view of a completely reconstructed single axon originating from the middle part of the left LRNm (fiber 5, exp 64). The reconstruction was made by using 96 serial coronal sections. This fiber ran through the ipsilateral IO, crossed the midline, passed through the contralateral IO, and then entered the cerebellum through the contralateral icp (see the inset at the bottom). Axon terminals were distributed in lobules II, III, IV, and V in the bilateral Cx (group 2B in Table 1). Note the predominant projection to the contralateral Cx and DCN including the VN. For abbreviations, see list. Scale bars = 1 mm, respectively.

In the Cx, the terminations of reconstructed axons were mostly seen in the vermis in the anterior lobe (fibers 1, 4, 5, 7, and 10), and often in lobule VI, especially VIa. Some fibers only innervated the vermal anterior lobe (fiber 5). Other termination areas of some fibers included lobules VII and VIII (fiber 7), Crus Ia, copula pyramidis, lobules IXa and b, and the paraflocculus (fiber 4).

Cortical primary collaterals sometimes sent terminal branches to a single lobule but more often to multiple lobules. Furthermore, terminal branches given off from each cortical primary collateral generally spread rather widely in the semiparasagittal plane (width, 400–2,000 μm, usually more than 1,000 μm) (see the lower panels in Figs. 9–11) within each lobule and extended to one to four adjacent lobules. In contrast, the spread of the terminal branches of a single primary collateral was relatively restricted in the transverse direction (mediolateral width, usually 300–650 μm). As a result, the distribution of terminals of a single LRN axon plotted in the coronal plane roughly showed a pattern of multiple longitudinal bands (see the upper panels in Figs. 9–11). Some cortical collaterals (e.g. some branches in Fig. 8) appeared to give rise to terminal branches that were distributed rather widely, up to about 1 mm in the transverse plane. However, these terminal branches did not spread solely in the transverse direction but also spread broadly in the longitudinal direction, which is not shown in the frontal view. Therefore, there seemed to be a general tendency for terminal branches given off from single cortical primary collaterals to exhibit longitudinal spread.

To reveal the nature of the longitudinal distribution of terminals in single LRN axons, terminal distributions of individual primary collaterals were analyzed in more detail, by using the completely reconstructed LRN axons. Figure 12 shows an example of such an analysis on the reconstructed LRN axon in Figure 9. The distances from the midline to individual terminals were measured and plotted on unfolded longitudinal strips of the vermal lobules in the Cx. In Figure 12A, two adjacent primary collaterals terminated in a longitudinal zone, which was

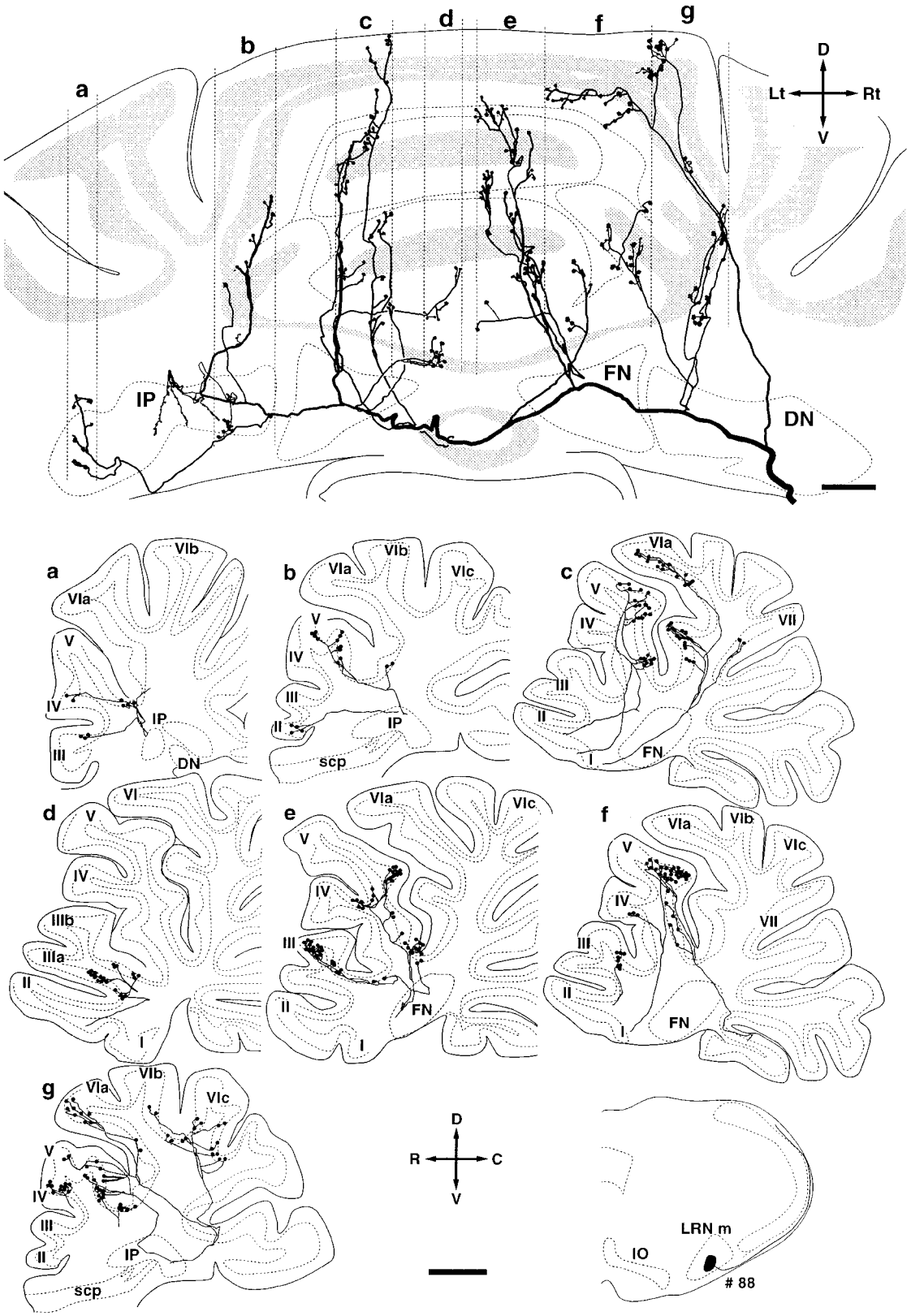

Fig. 9. Frontal (top) and lateral views (bottom) of a completely reconstructed single LRN axon originating from the caudal part of the right LRN (mostly LRNm; fiber 10, exp 88). This reconstruction was made by using 148 serial coronal sections. This fiber entered the cerebellum through the ipsilateral icp, projected to the bilateral Cx (lobules II through VII) and DCN (group 1B in Table 1), and formed a multiple longitudinal zonal projection pattern by its cortical arborescent collaterals. Bottom drawings show lateral views of individual collaterals as indicated in the top drawing with lowercase letters (**a–g**). The injection site is shown in the right inset at the bottom. Roman numerals indicate names of lobules. For abbreviations, see list. Scale bars = 0.5 mm (top); 1 mm (bottom).

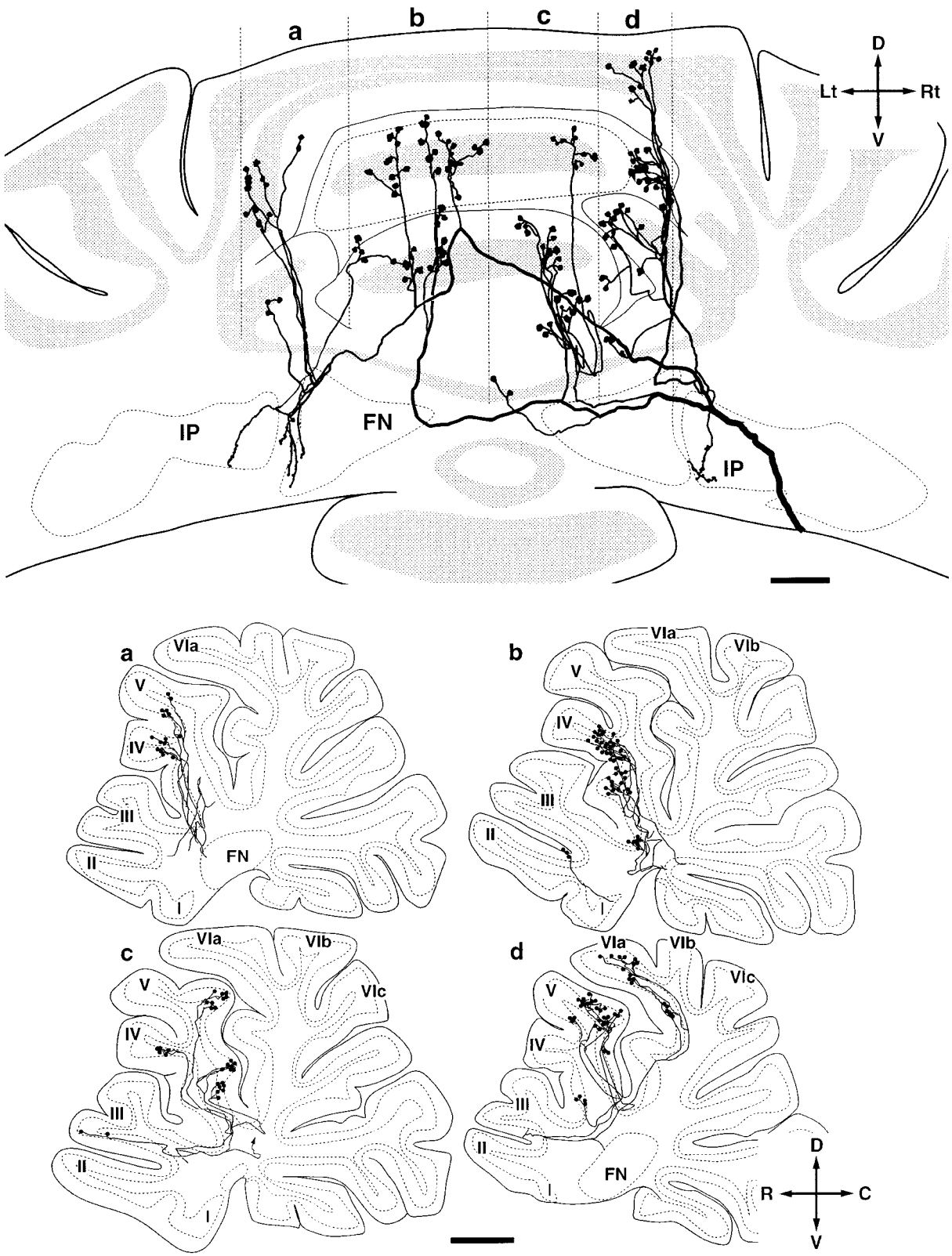

Fig. 10. Frontal (top) and lateral views (bottom) of a completely reconstructed single LRN axon originating from the dorsocaudal part of the right LRNm (fiber 6, exp 82). This reconstruction was made by using 123 consecutive coronal sections. The fiber ran through the ipsilateral icp and projected to the bilateral Cx and DCN (group 1B in Table 1). This fiber projected to lobules III through VIa and formed a multiple longitudinal zonal projection pattern by its cortical arborescent collaterals. Bottom drawings show lateral views of individual collaterals as indicated in the top drawing with lowercase letters (**a–d**). Roman numerals indicate names of lobules. For abbreviations, see list. Scale bars = 0.5 mm (top); 1 mm (bottom).

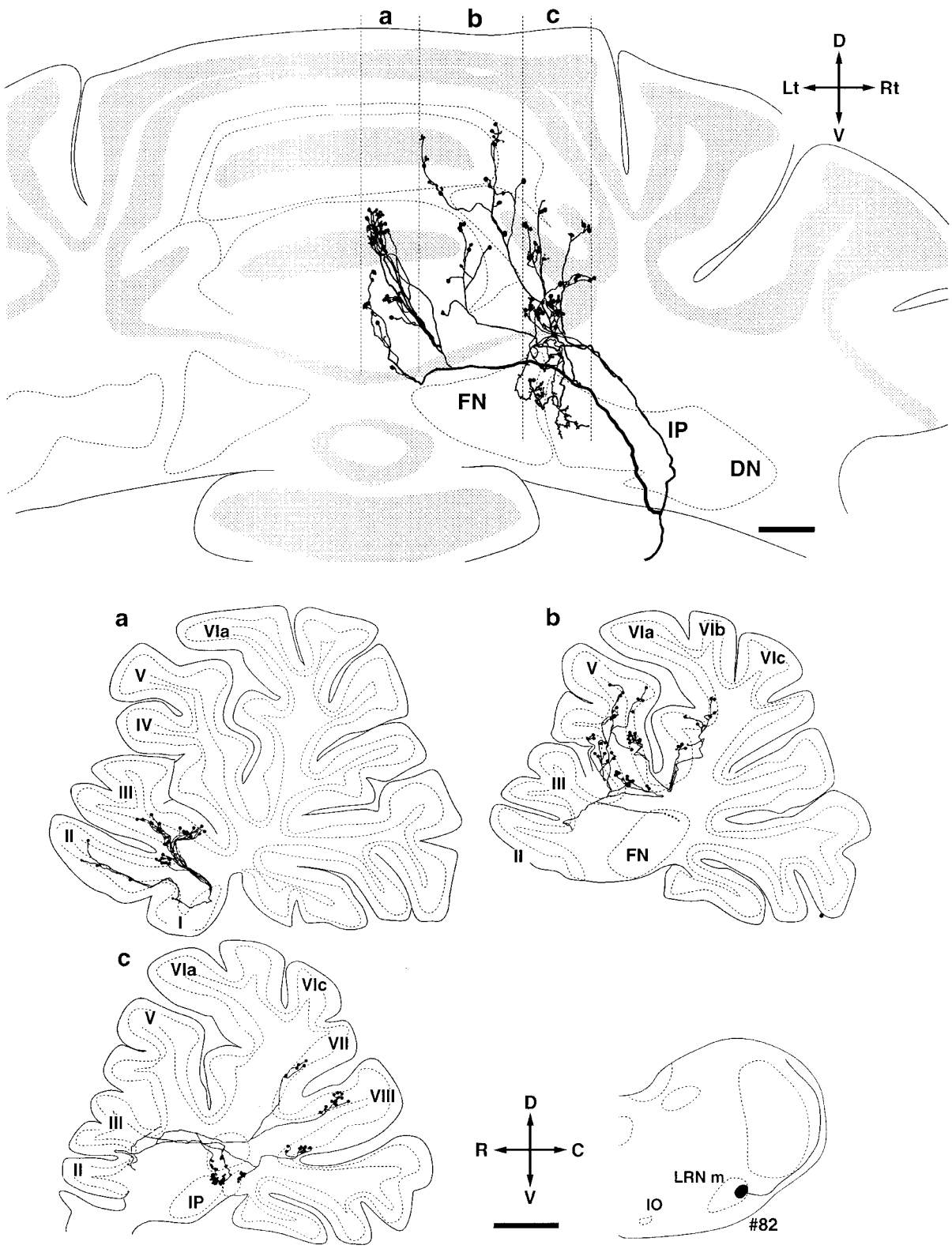

Fig. 11. Frontal (top) and lateral views (bottom) of a completely reconstructed single LRN axon originating from the dorsocaudal part of the right LRNm (fiber 7, exp 82). This reconstruction was made by using 146 consecutive coronal sections. The fiber ran through the ipsilateral icp and projected only to the ipsilateral Cx and DCN (group 1A in Table 1). The most medial cortical collaterals innervated lobules I, II, and III (top, **a**), the intermediate collaterals innervated lobules V and VI (top, **b**), and the most lateral collaterals innervated lobules VII and VIII (top, **c**). The bottom drawings show lateral views of individual collaterals as indicated in the top drawing with lowercase letters (a–c). The injection site is shown in the right inset at the bottom. Roman numerals indicate names of lobules. For abbreviations, see list. Scale bars = 0.5 mm (top); 1 mm (bottom).

TABLE 1. Classification of 11 Completely-Reconstructed Mossy Fibers Originating From the LRN

					Cx			DCN												
								ipsi						Contra						
Group	Specimen number	Axon diameter (μm)	Reconstructed axon	icp	ipsi (A)	contra (B)	A/B	VN	DN	IPa	IPp	FN	Total (A)	FN	IPa	IPp	DN	VN	Total (B)	A/B
1A	82	2.6	fiber 7	ipsi	137	0	—	—	0	21	53	17	91	0	0	0	0	—	0	—
	78	2.6	fiber 9	ipsi	123	0	—	—	0	22	46	15	83	0	0	0	0	—	0	—
1B	40	3.9	fiber 1	ipsi	74	53	1.40	—	0	70	0	0	70	31	0	77	0	—	108	0.65
	40	2.5	fiber 2	ipsi	107	62	1.73	—	0	0	45	35	80	0	24	49	0	—	73	1.10
	64	2.5	fiber 3	ipsi	82	65	1.26	—	0	0	44	12	56	22	0	21	0	—	43	1.30
	82	2.5	fiber 6	ipsi	93	67	1.39	—	0	0	49	0	49	0	0	59	0		59	0.83
	78	2.6	fiber 8	ipsi	103	47	2.19	0	0	0	8	0	8	11	0	0	0	17	28	0.28
	88	2.6	fiber 10	ipsi	152	67	2.26	—	0	0	0	0	0	0	7	89	0	—	96	0
	36	2.6	fiber 11	ipsi	113	70	1.61	0	0	0	67	0	67	83	0	0	0	35	118	0.86
2A	64	2.6	fiber 4	contra	0	84	—	0	0	0	0	0	0	50	0	27	0	43	120	0
2B	64	2.5	fiber 5	contra	85	110	0.77	0	0	0	0	7	7	0	0	107	80	76	263	0.03

labeled as zone c in Figure 9. In this zone, terminals that originated from one primary collateral were distributed in lobule V, and those from the other primary collateral were distributed in lobule VI where two clusters of terminals were slightly separated in lobule VIa and VId. The longitudinal spread of these terminals extended over 6.5 mm, whereas the mediolateral spread of each cluster of terminals was localized between 230 μm and 400 μm. Even as a whole, these terminals were well aligned in a single longitudinal strip less than 400 μm wide in the transverse plane. Similarly, Figure 12B shows the distribution of terminals of another primary collateral of the same axon (labeled as zone e in Fig. 9) on the unfolded cortical parasagittal strip. This collateral bifurcated into two main branches, of which one branch terminated in lobule III, and the other branch terminated in lobules IV and V. Although terminals were distributed widely along a parasagittal longitudinal strip (11.6 mm), the mediolateral spread of the terminals was restricted within 600 μm as a whole. As shown in this example, the general feature of the cortical distribution of terminals of a single LRN axon could be summarized as follows. Terminals belonging to one or sometimes two primary collaterals and spreading in a few lobules made a longitudinal zone in the parasagittal plane that was usually less than 500 μm wide in the transverse plane, and several such longitudinal zones of terminals were arranged in parallel in the mediolateral direction.

Morphology and distribution of collaterals terminating in the DCN and VN

All of the completely reconstructed LRN axons projected to the DCN by way of their collaterals (Figs. 8–11). Axon collaterals terminating in the DCN were given off from transverse stem axons (Fig. 13) or proximal parts of cortical primary branches (Fig. 8), and ran in the parasagittal direction. Each LRN axon had two to three (2.5 ± 0.5, n = 11) primary collaterals to the cerebellar (and vestibular) nuclei. Each of these primary collaterals was much thinner (diameter, 0.4–1.0 μm) than stem axons (diameter, 1.5–2.0 μm) and cortical branches and had a localized termination area in the DCN.

An arbor of a nuclear collateral could be sorted into a primary axon collateral and terminal branches, although the distinction between them was not definite. A primary axon collateral ran toward the target DCN in a relatively straight path without any branching when the branching point was far from the DCN (Figs. 8, 13). Within the DCN, a primary collateral bore several *en passant* swellings and had only one or two ramifications to produce several (usually one to four) terminal branches. Each terminal branch was usually about 200–500 μm long and bore frequent *en passant* swellings and sometimes short branchlets bearing a terminal swelling and occasionally a few *en passant* swellings (Figs. 13, 14). Usually, a single primary collateral terminated in only one target DCN (Fig. 13A, B), but sometimes sent terminal branches into two cerebellar nuclei or into both the cerebellar and vestibular nuclei (Fig. 13C). In addition, there were two types of terminals of LRN fibers in the DCN. Figure 14 shows these types of collaterals in the DCN. In most cases (Figs. 13, 14A), the diameter of the primary nuclear collaterals was about 0.5μm and that of the terminal branch was also about 0.5μm, whereas *en passant* and terminal swellings were 0.9 ± 0.3 μm in diameter (measured in 20 swellings) (type I collateral) (Fig. 14B). The rest of the primary nuclear collaterals (n = 2) given off from an LRN axon had a thick diameter (1.0μm at the primary collateral) and bigger swellings (diameter 1.7 ± 0.4 μm, measured in 20 swellings) (type II collateral) (Fig. 14C). There was no clear difference in the disposition of swellings or in the characteristics of arborization between these two types of collaterals.

Some thin collaterals with swellings in the DCN did not end within the DCN, but extended further in the rostral and ventral directions (nuclear collaterals in 4 of 11 LRN axons). In one case, a collateral extended to the LVN from within the FN (not shown). In other cases, a collateral extended to the LVN from within the IPp (Fig. 13C), or a collateral was extended to the area around the border

Fig. 12. Longitudinal distribution of axon terminals of single primary collaterals of a reconstructed LRN axon in the unfolded Cx (fiber 10, exp 88). **A:** Terminals of two primary collaterals (the same collaterals reconstructed in Fig. 9c) plotted on the unfolded Cx (left). Two terminals in lobule VII are not included in the unfolded strip, but they were located in the same parasagittal strip, even though they were far away from the other terminals. **B:** Terminals borne on a primary collateral (shown in Fig. 9e) plotted on unfolded lobules III–V (right). The rostrocaudal distance of the Cx was measured at the surface of the molecular layer on a reconstructed parasagittal section, and the locations of axon terminals in the granular layer were projected to the corresponding sites on the surface of the unfolded Cx. Arabic numbers attached to the portions of the folia correspond to those on the unfolded cortical parasagittal strips. Roman numbers indicate names of lobules. Note the narrow mediolateral and wide longitudinal distributions of terminals belonging to individual primary collaterals. For abbreviations, see list. Scale bars = 1 mm.

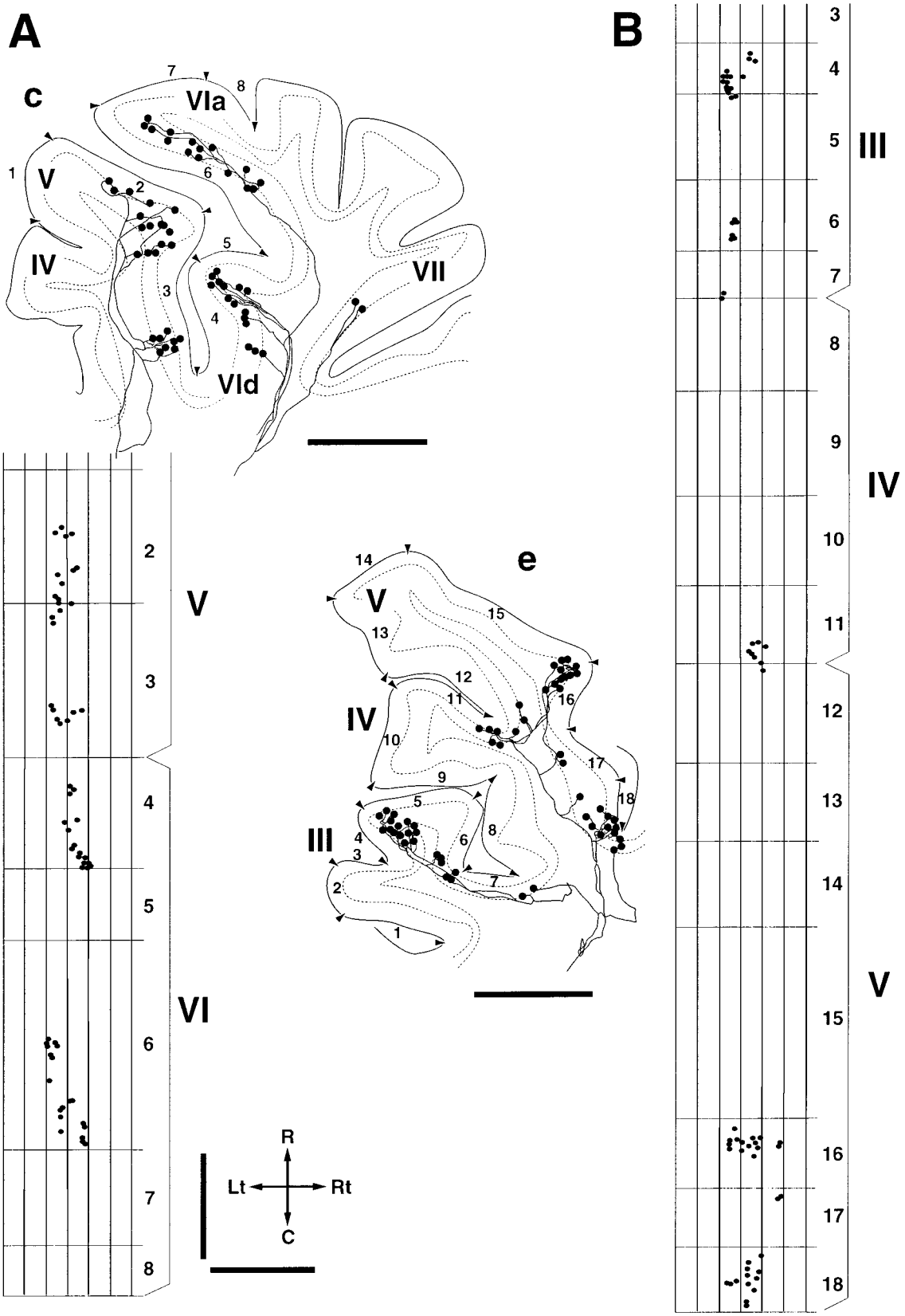

Figure 12

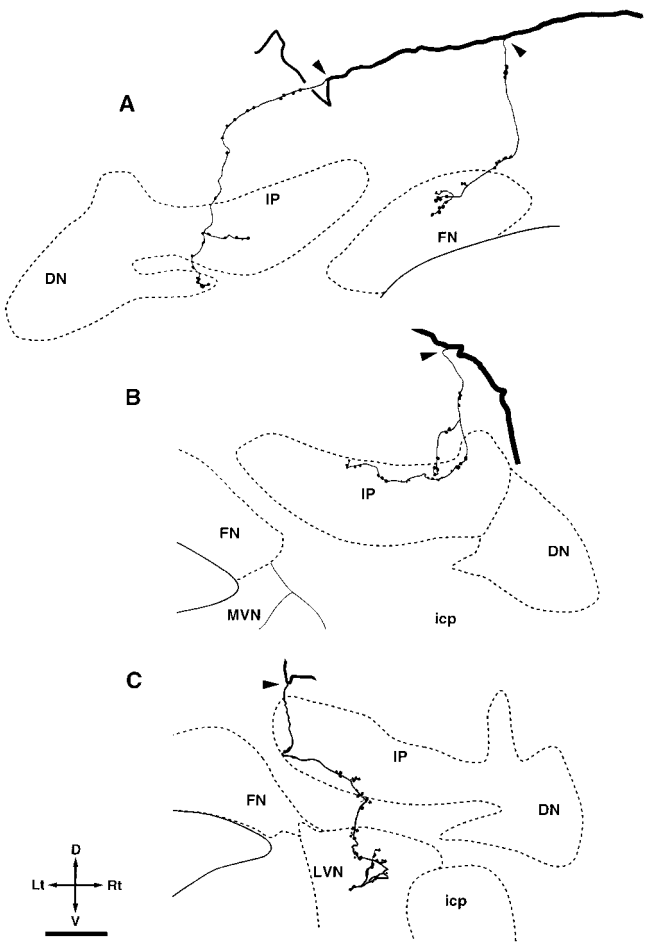

Fig. 13. Trajectories of collaterals terminating in the cerebellar nuclei (**A,B**) and a collateral terminating in both the cerebellar and lateral vestibular nuclei (**C**) in coronal sections. Arrowheads indicate branching points of collaterals from the stem axon. For abbreviations, see list. Scale bar = 0.5 mm.

between the LVN and superior vestibular nucleus (SVN) from the FN (not shown). All of the collaterals innervating the VN that were reconstructed in the present study were first given off from the transverse stem axon in the deep cerebellar white matter. After sending some terminal branches to the FN or interposed nucleus (IP), they entered the VN from the dorsal part. The dorsal part of the LVN was most often innervated (three of four) by these collaterals. The axons with these collaterals originated from the ventral part of the middle of the LRN (exp 36, 64, 72, and 78 in Fig. 1), which tended to have collaterals terminating in the VN. This area of the LRN contains passing SCT axons, but four axons with vestibular collaterals were identified as LRN axons (see previous section).

Relationship between cortical and nuclear projections in single LRN axons

Projection to the DCN was observed in all of the reconstructed LRN axons. LRN axons most often innervated the FN and IPp, and occasionally the DN and the IPa. There seemed to be a rough correspondence between the cortical and nuclear projections of single LRN axons that was compatible with the zonal arrangement in corticonuclear projection (Voogd et al., 1996). When an axon had a collateral in the FN, the same axon always had terminations on the vermis on the same side as the FN. However, LRN axons that projected to the vermis did not necessarily have axon collaterals to the FN (fibers 1, 2, 5, and 10, right side, Figs. 8, 9). When an axon had collateral(s) in the IP and the DN, the same axon often innervated the intermediate area, including the most lateral vermis and the hemisphere of the Cx, respectively (Figs. 9–11), although there were occasional exceptions (Fig. 8).

DISCUSSION

The present study revealed the entire trajectory of single mossy fibers originating from the LRN and extending to the Cx and DCN by reconstructing BDA-labeled axons on serial sections. Virtually all of the reconstructed LRN axons projected not only to the Cx as mossy fibers, but also to the DCN, including the VN, by their axon collaterals. None of the LRN neurons specifically projected to the DCN without projecting to the Cx; i.e., all of the axon terminals of LRN neurons in the DCN and VN were axon collaterals of mossy fibers projecting to the Cx. In general, axon collaterals in the DCN and VN had a simple branching pattern and a narrow projection area, whereas those in the Cx had a complex branching pattern and a wide mediolateral spread, usually bilaterally, with multiple longitudinal zones in multiple lobules.

It has long been known that projections of many cerebellar afferents take the form of mossy fibers, but most previous anatomic studies have examined the projection as a mass. Our group has so far succeeded in describing the detailed morphology of single functionally identified mossy fibers in the Cx (Krieger et al., 1985) and in the DCN (Shinoda et al., 1992, 1997) in the cat. However, the entire trajectory of mossy fibers in the cerebellum of a particular precerebellar nucleus neuron has not been previously revealed, partly because the cerebellum of the cat is too large to completely stain the entire trajectory of single axons. On the other hand, electrophysiologic studies have demonstrated axonal branchings of single LRN neurons to different cortical areas (Clendenin et al., 1974a–d). However, electrophysiologic studies are not necessarily capable of quantitatively analyzing all of the branches of mossy fibers and nuclear collaterals of single neurons. In these respects, the detailed comprehensive morphology of single mossy fibers demonstrated in the present study is innovative and will contribute significantly to future physiologic studies on the mossy fiber system.

Specificity of labeling LRN neurons

Injection of BDA into the LRN resulted in an inadvertent labeling of SCT axons. However, by tracing many axons to their cell bodies, we could establish a rather reliable criteria to distinguish between LRN axons and SCT axons (see Results) and could reconstruct the identified LRN axons. Because some SCT axons seemed to be too faintly labeled in the cerebellar peduncles to remain labeled up to their terminals, the high levels of extraneous labeling (13–33%) obtained very likely overestimated the actual labeling of SCT axons among LRN axons in the Cx and DCN. At any rate, we only used experiments in which there were much fewer labeled SCT axons than labeled LRN axons to map axon terminals in the present study

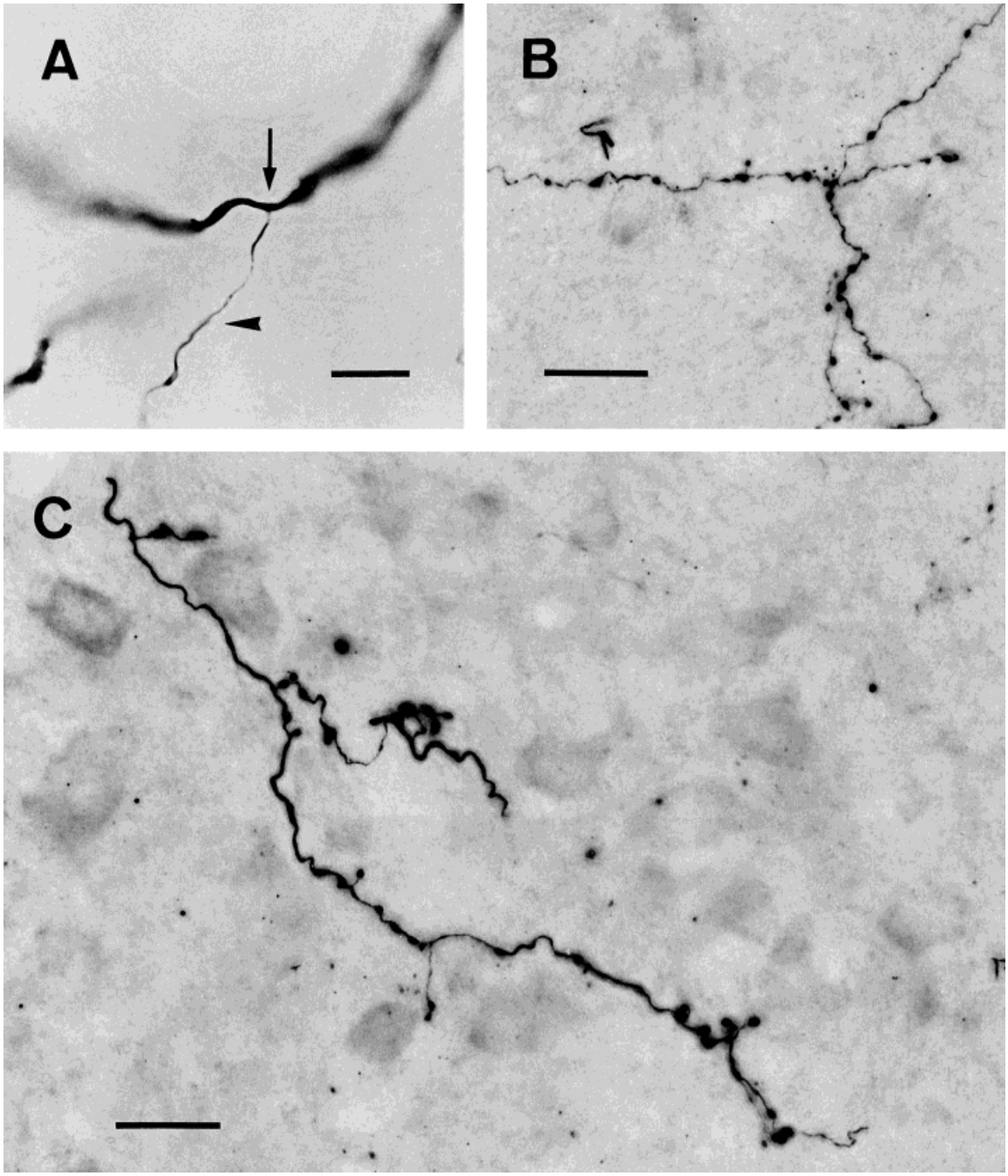

Fig. 14. Photomicrographs of a branching point of a collateral arising from a horizontally running stem axon of the LRN and terminating in the cerebellar nucleus (**A**) and terminals in the cerebellar nuclei (**B**,**C**). In A, an arrowhead indicates a thin cerebellar nuclear collateral arising from a thick stem axon (arrow) of a LRN neuron. A computer-aided autofocusing system was used in B and C. Scale bars = 10 μm in A; 2 μm in B,C.

(Figs. 3–6). Previous studies that used anterograde tracing methods did not consider extraneous labeled SCT axons, except for the study by Matsushita and Ikeda (1976), but the tracers used such as radioactive amino acids (Künzle, 1975; Chan-Palay et al., 1977) and *Phaseolus vulgaris* leucoagglutinin (PHA-L) (Ruigrok et al., 1995), may be much less likely to be taken up by passing fibers or collateral terminals.

Characteristics of the projection of single axons of LRN neurons

The cerebellar cortical projection of single LRN axons is generally characterized by broadness of the termination areas, which stands in sharp contrast to the single zonal projection of olivocerebellar axons (Sugihara et al., 1997). Single LRN axons simultaneously projected to different

areas in mediolateral locations in several lobules, often bilaterally, which suggests that there is significant overlap of the termination areas of single axons originating from within injection sites. Similar broadness of cortical innervation has been suggested in axons of other mossy fiber systems such as the cerebellar projection from the pontine nucleus (Shinoda et al., 1992).

Virtually all of the LRN axons that were reconstructed in the present study had collaterals terminating in the DCN, and also in the VN in some cases. This is the first mossy fiber system in which virtually all of the cerebellar cortical projection neurons are shown to have axon collaterals to the DCN. However, a high incidence of nuclear projection by means of axon collaterals cannot be generalized to all mossy fiber systems, because many mossy fibers originating from the pontine nucleus lack nuclear collaterals (Shinoda et al., 1992). Virtually all the entire cerebellar nuclear projection from the LRN was by means of thin collaterals given off from stem axons or primary cortical collaterals. Previous anterograde or retrograde studies did not identify whether nuclear projections of LRN neurons are by means of collaterals of mossy fibers or if there are specific nuclear-projecting neurons. Because most of the reconstructed LRN axons originated from the LRNm, we cannot discuss in detail the topographical relationship in LRN-nuclear projection as elaborated in a retrograde labeling study (Parenti et al., 1996). However, it is very clear that the topographical relationship in LRN-nuclear projection was much weaker and vaguer than that in the olivonuclear projection (Van der Want et al., 1989; Sugihara et al., 1996), in which neurons in a subdivision of the IO project to a relatively localized area in one of the cerebellar nuclei. This is partly because single LRN axons have multiple nuclear collaterals projecting to more than one cerebellar nuclei, and multiple cortical collaterals that spread rather widely in the transverse plane, whereas single IO neurons have multiple collaterals that spread in a very narrow longitudinal zone in the Cx (Sugihara et al., 1997).

Among our 29 completely reconstructed LRN axons, four axons had collaterals terminating in the VN. The dorsal portion of the LVN was most often innervated by LRN axons, which was consistent with the results of mass PHA-L labeling (Ruigrok et al., 1995), and primary collaterals innervating the VN always innervated the DCN. These collaterals extended ventrally from within the cerebellum, as suggested by a previous mass labeling study (Ruigrok et al., 1995). The three cerebellar nuclei and the dorsal LVN, to which LRN axons project, receive Purkinje inhibition, but the ventral LVN does not (Eccles et al., 1967). These findings may reflect a close relationship between the vestibular and cerebellar nuclei with regard to both ontogeny and phylogeny.

Area-dependent or neuron-dependent differences in LRN projection

The results of single axon reconstructions (Figs. 8–11) showed that the cerebellar projection from the LRNm was generally bilateral, predominantly in the vermis of the anterior lobe (especially lobules IV and V), lobule VI, and the paramedian lobule in the hemisphere, and less in lobules VII and VIII in the intermediate area. This result is roughly consistent with the results of previous anatomic studies, which showed that the LRNm mainly projects to lobules IV and V, whereas the LRNp and the cells located at the border between the LRNm and LRNp project to lobules II and III (Hrycyshyn et al., 1982; Ruigrok and Cella, 1995). A clear area-dependent difference in LRN-Cx projection was seen only in the dorsolateral part of the caudal LRNm (exp 82), although the injections extended from the rostromedial LRNm to the caudal LRNm. In this experiment, terminals were almost exclusively localized ipsilaterally, whereas the cerebellar innervation was bilateral in all of the other experiments. This finding seemed to be consistent with the results that the dorsolateral part of the caudal LRNm receives input from an ipsilateral distal forelimb and projects exclusively to the ipsilateral Cx (Clendenin et al., 1974a,d), and that no clear topographical subdivisions have been reported in projections from different areas within the LRNm, except for its dorsolateral part (Clendenin et al., 1974a; Dietrichs and Walberg, 1979; Hrycyshyn et al., 1982). However, some topographical projection has been shown among the three subdivisions of the LRN, i.e., LRNm, LRNp, and LRNst (Brodal, 1943; Ruigrok and Cella, 1995).

Abundant terminals were observed in the FN and medial portions of the IPa and IPp. This result is partly consistent with the retrograde labeling study by Parenti et al. (1996). They showed that the DN received a projection from the dorsomedial part of the rostral LRN, into which we could not inject BDA, and distinguished the intermedioventral and caudal LRN and dorsolateral part of the middle LRN, with the former projecting to the FN and the latter to the IP. The present analysis of single axon morphology has revealed the existence of multiple axon collaterals of single LRN neurons projecting to more than one cerebellar or vestibular nucleus. This is the first mossy fiber system in which single axons have been shown to innervate multiple cerebellar nuclei.

Multiple longitudinal zonal projection of single LRN neurons in the Cx

The injection of large volumes of BDA into the LRN revealed multiple longitudinal zones of mossy fiber terminals in the Cx. This finding is consistent with the results obtained in the rat and the cat by Künzle (1975) and Chan-Palay et al. (1977), by using an autoradiographic method, and by Ruigrok and Cella (1995) by using PHA-L. One of the most important findings in this study is the existence of multiple zonal projection of single LRN axons in the Cx. This projection is in a sharp contrast with the projection of the IO, which also shows a multiple longitudinal zonal pattern, when labeled by the mass injection of an anterograde tracer (Chan-Palay et al., 1977; Van der Want et al., 1989). However, at the level of single axons, the cortical projection is generally localized within a single longitudinal zone in the climbing fiber system (Sugihara et al., 1997), whereas it is multizonal in the LRN mossy fiber system. The present multiple zonal projection of a single mossy fiber may not necessarily contradict the patchy or fractured representation of receptive fields of the facial area (Shambes et al., 1978), because terminals of single axons seemed to be arranged into clusters within each longitudinal zone (Fig. 12). The important point of the terminal distribution pattern of a single LRN axon is that terminals in different lobules originating from single or adjacent primary collaterals, even though they are separated widely, are localized in a parasagittal longitudinal zone that is restricted to less than 500 μm wide in the

mediolateral direction. This organization is very similar to the organization of a single olivocerebellar axon in the Cx. Therefore, this longitudinal zonal organization should be a basic and common organization for both the climbing and mossy fiber systems.

One of the important remaining questions is how the longitudinal arrangement of LRN projection is related to zonal components A, B, C1, C2, C3, D0, D1, and D2, which were identified with olivocerebellar and corticonuclear projections (Groenewegen and Voogd, 1977; Buisseret-Delmas and Angaut, 1993; Voogd, 1995). We attempted in vain to correlate these zones with the present zones of LRN terminals by combining acetylcholine esterase staining and the present staining, because the zones visualized by acetylcholine esterase staining appeared mainly in the posterior vermis. The relationship between the multiple zones of LRN projection and zebrin-defined zones has been briefly addressed by Ruigrok and Cella (1995), and the zones defined by the different methods seem to correspond well with each other. Thus, the functional significance of cerebellar compartmentalization, which has so far been studied from the perspective of labeling molecular marker-specific Purkinje cells and labeling olivocerebellar and corticonuclear projections, could be also considered from the viewpoint of mossy fiber projections.

Functional significance of axonal branching patterns of single LRN axons

Excitatory mossy fiber inputs to the Cx are relayed by granule cells and parallel fibers to reach Purkinje cells. Although a parallel fiber spreads in the transverse direction, the most effective input from the parallel fiber is given to Purkinje cells just above the given granule cell through synapses formed by the parallel fiber (Eccles et al., 1967). Therefore, the zonal projection of a single LRN axon may be functionally significant in conveying an excitatory input to Purkinje cells in that specific zone.

Individual LRN axons projected to multiple lobules in both the hemisphere and the vermis, and even often bilaterally. Therefore, cerebellar cortical areas innervated by a single mossy fiber from the LRN may not necessarily be related to each other in terms of their functional roles. Thus, an important question is what is the role of LRN axons that presumably send specific information to different cortical areas (Clendenin et al., 1974b). Concerning the nuclear projection, it is obvious that the cortical and nuclear projections of any single reconstructed LRN axon did not exactly follow the so-called corticonuclear topographical relationship, because the cortical projection generally spread more widely in the transverse direction than the nuclear projection (Figs. 8–11, 13). Thus, this situation does not exactly correspond to the classic microcomplex scheme of Ito (1984), in which the nuclear inputs by a mossy fiber collateral and by a Purkinje cell that receives the same mossy fiber input through granule cells converge onto the same target nuclear output neuron. The nuclear collaterals of mossy fibers are important in activating nuclear neurons as a source for the excitation of their target neurons (Shinoda et al., 1992, 1997). To understand the functional interactions at nuclear efferent neurons between Purkinje cell inputs in widely distributed cortical areas innervated by a single mossy fiber and nuclear inputs by a collateral of the same mossy fiber, we need more detailed information about how single Purkinje cells spread in the DCN, how Purkinje cells in different cortical areas send their information to the DCN, and how that information is integrated as an output in the DCN. Furthermore, it would also be useful for understanding the functional mechanism of mossy fiber systems to clarify the similarities and the differences in mossy fibers in other systems, such as spinocerebellar and cuneocerebellar systems.

ACKNOWLEDGMENTS

We thank Mr. M. Takada for his photographic assistance and Dr. K. Miura of for his support of the computer-aided dynamic focusing system. Y.S. received support from the Core Research for Evolutional Science and Technology of the Japan Science and Technology Corporation. I.S. and Y.S. received grants-in-aid for scientific research from the Ministry of Education, Science, and Culture of Japan. H.-S.W. received a research grant from the Sasakawa Health Science Foundation and a scholarship from the Iwaki Scholarship Foundation.

LITERATURE CITED

Alstermark B, Isa T, Tantisira B. 1990. Projection from excitatory C3-C4 propriospinal neurons to spinocerebellar and spinoreticular neurons in the C6-Th1 segments of the cat. Neurosci Res 8:124–130.

Andersson G, Oscarsson O. 1978. Climbing fiber microzones in cerebellar vermis and their projection to different groups of cells in the lateral vestibular nucleus. Exp Brain Res 32:564–579.

Brodal A. 1943. The cerebellar connections of the nucleus reticularis lateralis (nucleus funiculi lateralis) in rabbit and cat experimental investigations. Acta Psychiatr Scand 18:171–233.

Brodal A. 1981. Neurological anatomy, 3rd ed, New York: Oxford University Press.

Bruckmoser P, Hepp M-C, Wiesendanger M. 1970. Cortical influence on the single neurons of the lateral reticular nucleus of the cat. Exp Neurol 26:239–252.

Buisseret-Delmas C, Angaut P. 1993. The cerebellar olivocorticonuclear connections in the rat. Prog Neurobiol 40:63–87.

Chan-Palay V, Palay SL, Brown JT, Van Itallie C. 1977. Sagittal organization of olivocerebellar and reticulocerebellar projections: autoradiographic studies with 35S-Methionine. Exp Brain Res 30:561–576.

Clendenin M, Ekerot C-F, Oscarsson O, Rosén I. 1974a. The lateral reticular nucleus in the cat I Mossy fibre distribution in cerebellar cortex. Exp Brain Res 21:473–486.

Clendenin M, Ekerot C-F, Oscarsson O, Rosén I. 1974b. The lateral reticular nucleus in the cat. II. Organization of component activated from bilateral ventral flexor reflex tract (bVFRT). Exp Brain Res 21:487–500.

Clendenin M, Ekerot C-F, Oscarsson O. 1974c. The lateral reticular nucleus in the cat. III. Organization of component activated from ipsilateral forelimb tract. Exp Brain Res 21:501–513.

Clendenin M, Ekerot C-F, Oscarsson O, Rosén I. 1974d. Functional organization of two spinocerebellar paths relayed through the lateral reticular nucleus in the cat. Brain Res 69:140–143.

Dietrichs E, Walberg F. 1979. The cerebellar projection from the lateral reticular nucleus as studied with retrograde transport of horseradish peroxidase. Anat Embryol 155:273–290.

Eccles JC, Ito M, Szentágothai J. 1967. The cerebellum as a neuronal machine. Berlin-Heidelberg-New York: Springer-Verlag. p 227–261.

Ekerot C-F, Oscarsson O. 1975. Inhibitory spinal paths to the lateral reticular nucleus. Brain Res 99:157–161.

Futami T, Shinoda Y, Yokota J. 1979. Spinal axon collaterals of corticospinal neurons identified by intracellular injection of horseradish peroxidase. Brain Res 164:279–284.

Gerrits NM, Voogd J. 1987. The projection of the nucleus reticularis tegmenti pontis and adjacent regions of the pontine nuclei to the central cerebellar nuclei in the cat. J Comp Neurol 258:52–62.

Grant G. 1962. Spinal course and somatotopically localized termination of the spinocerebellar tract. An experimental study in the cat. Acta Physiol Scand 56(Suppl)193:1–45.

Groenewegen HJ, Voogd J. 1977. The parasagittal zonation within the olivocerebellar projection. I. Climbing fiber distribution in the vermis of the cat cerebellum. J Comp Neurol 174:417–488.

Hrycyshyn AW, Flumerfelt BA, Anderson WA. 1982. A horseradish peroxidase study of the projections from the lateral reticular nucleus to the cerebellum in the rat. Anat Embryol 165:1–18.

Ito M. 1984. The Cerebellum and Neural Control. New York: Raven Press.

Ito M, Orlov I, Yamamoto M. 1982. Topographical representation of vestibulo-ocular reflex in rabbit cerebellar flocculus. Neuroscience 7:1657–1664.

Itoh K, Konishi A, Nomura S, Mizuno N, Nakamura Y, Sugimoto T. 1979. Application of coupled oxidation reaction to electron microscopic demonstration of horseradish peroxidase: cobalt-glucose oxidase method. Brain Res 175:341–346.

Kapogianis EM, Flumerfelt BA, Hrycyshyn AW. 1982. Cytoarchitecture and cytology of the lateral reticular nucleus in the rat. Anat Embryol 164:229–242.

Korneliussen HK. 1968. On the morphology and subdivision of the cerebellar nuclei of the rat. J Hirnforsch 10:109–122.

Krieger C, Shinoda Y, Smith AM. 1985. Labelling of cerebellar mossy fiber afferents with intra-axonal horseradish. Exp Brain Res 59:414–417.

Künzle H. 1973. The topographic organization of spinal afferents to the lateral reticular nucleus of the cat. J Comp Neurol 149:103–116.

Künzle H. 1975. Autoradiographic tracing of the cerebellar projections from the lateral reticular nucleus in the cat. Exp Brain Res 22:255–266.

Larsell O. 1952. The morphogenesis and adult pattern of the lobules and fissures of the cerebellum of the white rat. J Comp Neurol 97:281–356.

Matsushita M, Ikeda M. 1976. Projections from the lateral reticular nucleus to the cerebellar cortex and nuclei in the cat. Exp Brain Res 24:403–421.

Matsushita M, Yaginuma H. 1995. Projections from the central cervical nucleus to the cerebellar nuclei in the rat, studied by anterograde axonal tracing. J Comp Neurol 353:234–246.

Mihailoff GA. 1993. Cerebellar nuclear projections from the basilar pontine nuclei and nucleus reticularis tegmenti pontis as demonstrated with PHA-L tracing in the rat. J Comp Neurol 330:130–146.

Oscarsson O. 1976. Spatial distribution of climbing and mossy fibre inputs into the cerebellar cortex. In: Creutzfeldt O, editor. Experimental brain research supplement 1: afferent and intrinsic organization of laminated structures in the brain. Berlin: Springer Verlag. p 36–42.

Oscarsson O, Rosén I. 1966. Response characteristics of reticulocerebellar neurones activated from spinal afferents. Exp Brain Res 1:320–328.

Palay SL, Chan-Palay V. 1974. Cerebellar cortex. Cytology and organization. Berlin: Springer-Verlag.

Parenti R, Cicirata F, Pantò MR, Serapide MF. 1996. The projection of the lateral reticular nucleus to the deep cerebellar nuclei. An experimental analysis in the rat. Eur J Neurosci 8:2157–2167.

Ramón y Cajal S. 1911. Histologie du Systeme Nerveux de l'Homme et des Vertebrés, Vol II. Paris: Maloine.

Rubertone LA, Mehler WR, Voogd J. 1995. The vestibular nuclear complex. In: Paxinos G, editor. The rat nervous system, 2nd ed. Sydney: Academic Press. p 773–796.

Ruigrok TJH, Cella F. 1995. Precerebellar nuclei and red nucleus. In: Paxinos G, editor. The rat nervous system, 2nd ed. Sydney: Academic Press. p 277–308.

Ruigrok TJH, Cella F, Voogd J. 1995. Connections of the lateral reticular nucleus to the lateral vestibular nucleus in the rat. An anterograde tracing study with Phaseolus vulgaris leucoagglutinin. Eur J Neurosci 7:1410–1413.

Sato Y, Kawasaki T, Ikarashi K. 1983. Afferent projections from the brainstem to the floccular three zones in cats. II. Mossy fiber projections. Brain Res 272:37–48.

Shambes GM, Beermann DH, Welker W. 1978. Multiple tactile areas in cerebellar cortex: another patchy cutaneous projection to granule cell columns in rats. Brain Res 157:123–128.

Shinoda Y, Yokota J, Futami T. 1981. Divergent projection of individual corticospinal axons to motoneurons of multiple muscles in the monkey. Neurosci Lett 23:7–12.

Shinoda Y, Ohgaki T, Futami T. 1986. The morphology of single lateral vestibulospinal tract axons in the lower cervical spinal cord of the cat. J Comp Neurol 249:226–241.

Shinoda Y, Sugiuchi Y, Futami T, Izawa R. 1992. Axon collaterals of mossy fibers from the pontine nucleus in the cerebellar dentate nucleus. J Neurophysiol 67:547–560.

Shinoda Y, Sugiuchi Y, Futami T. 1993. Organization of excitatory inputs from the cerebral cortex to the cerebellar dentate nucleus. Can J Neurol Sci 20(Suppl 3):S19–S28.

Shinoda Y, Izawa Y, Sugiuchi Y, Futami T. 1997. Functional significance of excitatory projections from the precerebellar nuclei to interpositus and dentate nucleus neurons for mediating motor, premotor and parietal cortical inputs. In: deZeeuw CI, Strata P, Voogd J, editors. The cerebellum: from structure to control. Progress in Brain Research, vol 114. Amsterdam: Elsevier. p 193–207.

Snider RS. 1950. Recent contributions to the anatomy and physiology of the cerebellum. Arch Neurol Psychiatry 64:196–219.

Sugihara I, Wu H, Shinoda Y. 1996. Morphology of axon collaterals of single climbing fibers in the deep cerebellar nuclei of the rat. Neurosci Lett 217:33–36.

Sugihara I, Wu H-S, Shinoda Y. 1997. Projection of climbing fibers originating from single olivocerebellar neurons in the rat cerebellum. Soc Neurosci Abstr 23:1830.

Swanson LW. 1992. Brain maps: structure of the rat brain. Amsterdam: Elsevier.

Van der Want JJL, Wiklund L, Guegan M, Ruigrok T, Voogd J. 1989. Anterograde tracing of the rat olivocerebellar system with *Phaseolus vulgaris* leucoagglutinin (PHA-L). Demonstration of climbing fiber collateral innervation of the cerebellar nuclei. J Comp Neurol 288:1–18.

Voogd J. 1964. The cerebellum of the cat. Structure and fibre connexions. Assen: Van Gorcum & Comp NV.

Voogd J. 1995. Cerebellum. In: Paxinos G, editor. The rat nervous system, 2nd ed. Sydney: Academic Press. p 309–350.

Voogd J, Jaarsma D, Marani E. 1996. The cerebellum, chemoarchitecture and anatomy. In: Swanson LW, Björklund A, Hökfelt T, editors. Integrated systems of the CNS, Part III. Cerebellum, basal ganglia, olfactory system. Handbook of chemical neuroanatomy, Vol 12. Amsterdam: Elsevier. p 1–369.

Walberg F. 1952. The lateral reticular nucleus of the medulla oblongata in mammals. J Comp Neurol 96:283–343.